CHAPTER 4

FATIGUE-INDUCED DAMAGE AND BRIDGE LIFE FOR DIFFERENT STRESS BANDS OF AN EXISTING RAIL-CUM-ROADWAY BRIDGE

4.1 General

The period around the 19th to the 20th century witnessed a rapid evolution in transport systems, marked by the construction of numerous riveted steel bridges in various countries. These days, this is typically thought of as their design working life, which was not factored in during the bridge construction process. Many of these historic bridges have undergone multiple phases of repair or reinforcement, prompted by changes in service requirements. Despite such interventions, visible signs of deterioration or fatigue are often absent.

Nevertheless, it is advisable to conduct a thorough assessment of these bridges, especially before making decisions on costly repairs, retrofitting, or protection systems. The sheer volume of these aging bridges makes replacement due to the approaching "design life" impractical, given the constraints of available funds.

Due to the cyclical nature of traffic loads and the resulting vulnerability of railway bridges to time-dependent fatigue damage, it is now more crucial than ever to assess the remaining fatigue life of the existing railway bridges for uninterrupted services, especially when making decisions about structure replacement and other significant retrofits. However, the increased axel load, traffic volume, and bridge corrosion deterioration make this task challenging.

There are three types of bridges, namely minor, major and important bridges in Indian railways. Existing bridge is an important bridge type as per criteria laid down by (RDSO 2013).

4.2 Bridge description

Initially, the bridge was constructed in the year 1887, and traffic has been plying over the bridge since 1888 (Walton 1890). Substructure of the bridge is not changed since 1887. The superstructure of the rail cum road bridge was changed in 1947. The bridge over the Ganga River is a double-decker (2-lane roadway at top and double-track railway at bottom) riveted steel truss bridge near Kashi station in the Pt. DD Upadhyaya -Varanasi section that belongs to the northern railway zone of Indian railways shown in Figure 4.1(a). The line diagram of the overall bridge is represented in Figure 4.1(b).

Figure 4.1(a): Steel railway bridge in the Pt. DD Upadhyaya -Varanasi section

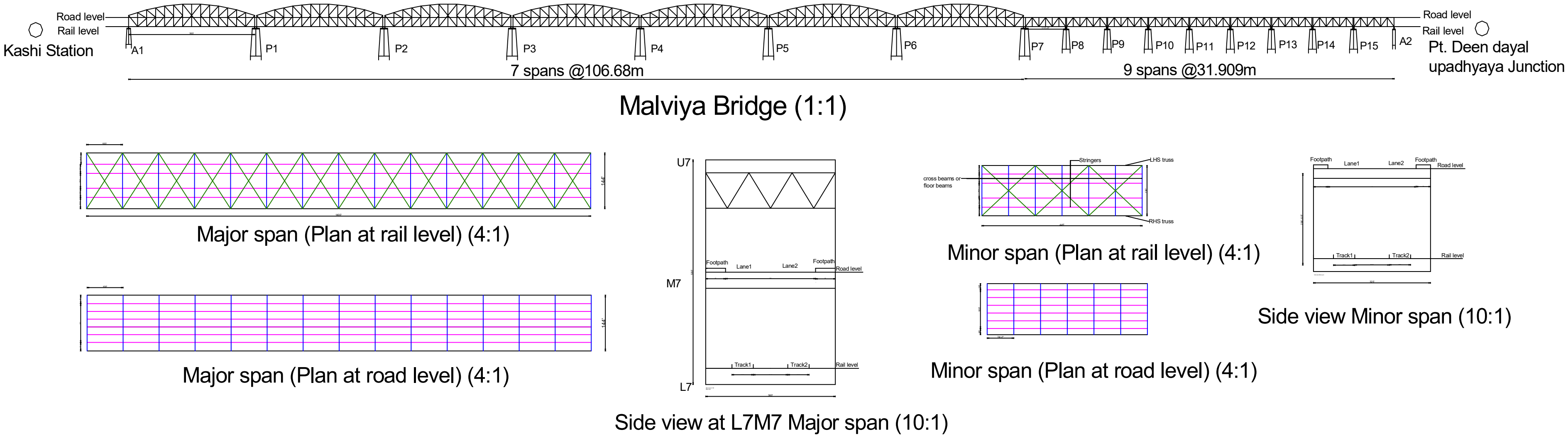

Figure 4.1(b): Schematic line diagram of the overall bridge

Roadway of the bridge is on India's National Highway. Railway lines between Pt. DD Upadhyaya junction and Varanasi junction, and the bridge's location are shown in Figure 4.2. There are three types of bridges, namely minor, major, and important bridges in Indian railways. The existing bridge is an important bridge type as per criteria laid down by (RDSO 2013). Riveted built up steel sections consist of plate and angles are used as bridge members. The authors conducted site visits to get dimensional specifications of the existing bridge. Railway officials also provided few drawings of the bridge. The Existing bridge has a seven major spans of 106.68m length and nine Minor spans of 33.91m (7x106.68 m + 9x33.91 m spans). Length is measured from centre to centre of bearing. The total length of bridge is more than one kilometre. The bridge features a steel superstructure, reinforced cement concrete bed blocks, and rocker-roller bearings. Over a well foundation, brick masonry piers were built.

Figure 4.2. Railway lines between Varanasi junction and Pt. DD Upadhyaya junction (Bridge location: 25°19'18.5"N 83°02'06.5"E) (reproduced from Indian railways, n.d.)

4.3 Loading and traffic details

4.3.1 Indian railway loading

As per (RDSO 2014), there are different types of loading used by Indian railways. Broad Gauge Main Line (BGML) loading, Revised Broad Gauge (RBG) loading, and Modified Broad Gauge (MBG) loading documented in 1926, 1975, and 1987, respectively. Then CC, CC + 6 + 2T and CC + 8 + 2T loadings are used in Indian railways. In CC + a + bT: CC represent carrying capacity, a denotes additional load over CC, and b depicts tolerance margin. In 2008, to fulfil increased loading requirement, 25T loading was documented. The latest loading is 32.5T, also known as dedicated freight corridor loading (DFC loading). Each successive loading has higher axle load than its predecessor one. Although loading adopted in the railway tracks in the later years after their initial documentation provided in (RDSO 2014). For instance, guidelines for DFC loading (32.5T loading) was provided in the year 2017 but till date, this loading is not used over railway tracks by Indian railways. There is a difference of approximately 2.0 ton in axle loads of train 25T-L and CC+8+2T-L, but axle spacing of trains locomotives and wagons have major differences. Wagons of all empty trains like BGML-E, RBG-E, MBG-E, CC+8+2T-E, 25T-E and 32.5T-E have same axle load. Only axle spacing varies for all empty trains. 32.5T loading is also called dedicated freight corridor (DFC) loading. It is the heaviest freight loading which is scheduled to be run over bridges in Indian railways in the future.

4.3.2 Bridge traffic details

Loading over the bridge is taken from 1948 onwards for the remaining life assessment. 25T railway loading is proposed over the bridge which is having a higher axle load than current loading CC+8+2T and past loadings like MBG, RBG, and BGML loading. Figure 4.3 depicts the loading arrangement for various types of passenger and freight trains (data from RDSO 2014) used in the herein study for fatigue analysis of the bridge. Since traffic density is increasing day by day, same has been incorporated in future load estimation over the bridge. Cumulative traffic density for concerned bridge is illustrated in Figure 4.4. At road level, IRC Class-A loading is applied by maintaining clear distance of 18.5m between two adjacent vehicles in the same lane. For Minor span, two IRC-A vehicles were applied at road level; in the case of major span, three IRC class-A vehicles applied at clear spacing of 18.5m in the STAAD model.

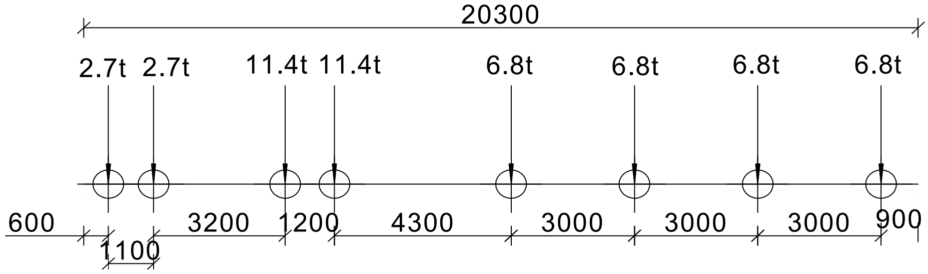

(a) IRC class-A vehicle

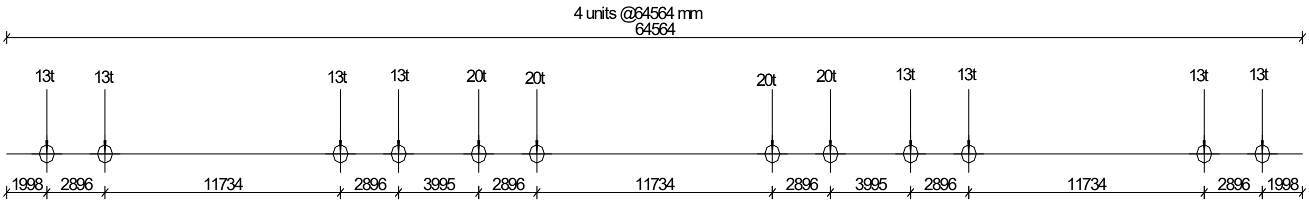

(b) PT-EMU

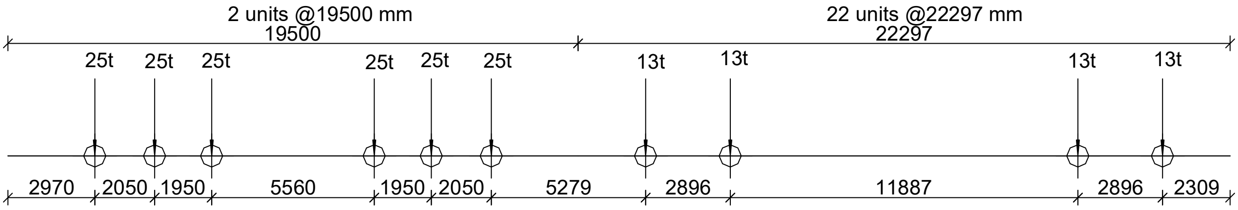

(c) PT-22

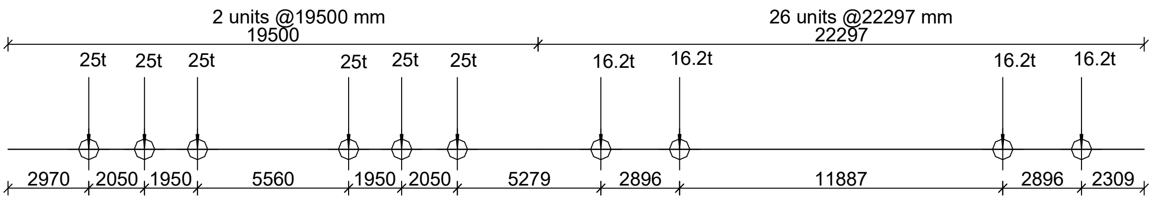

(d) PT-26

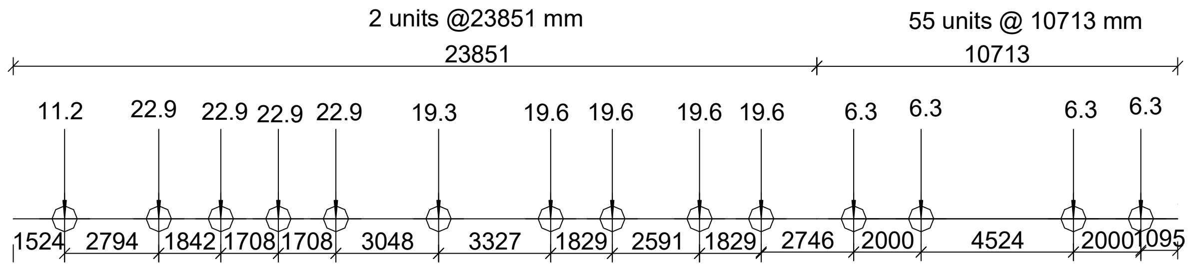

(e) BGML-E

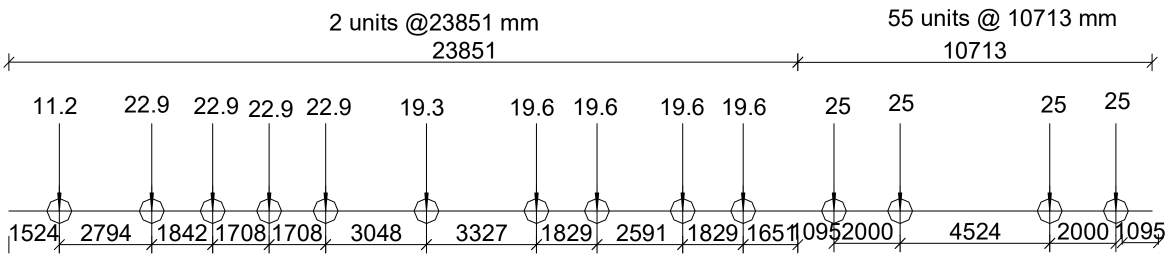

(f) BGML-L

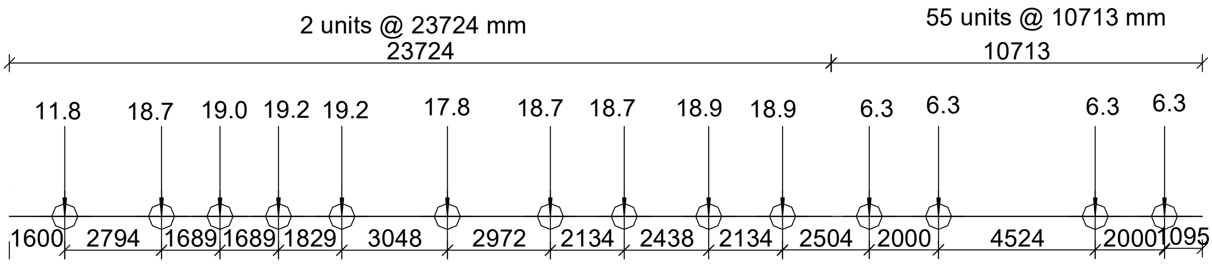

(g) RBG-E

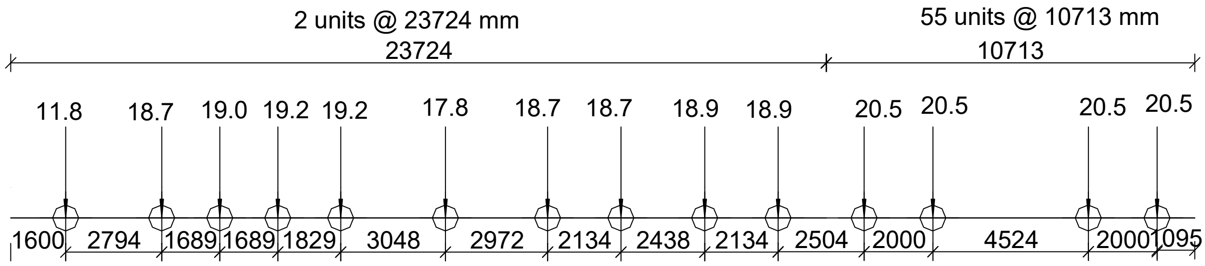

(h) RBG-L

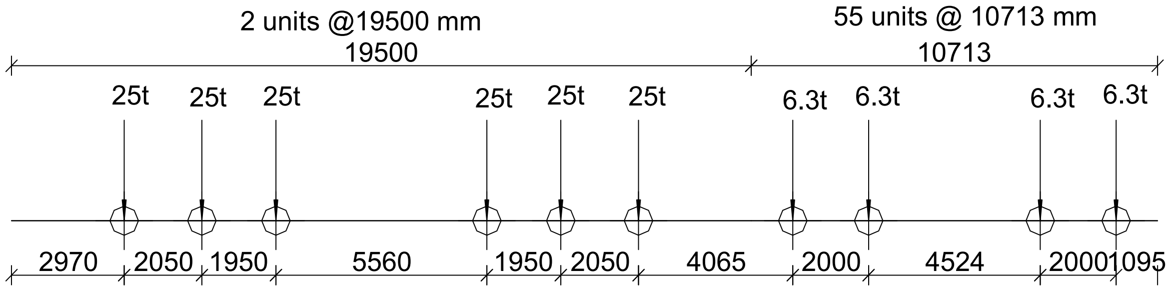

(i) MBG-E

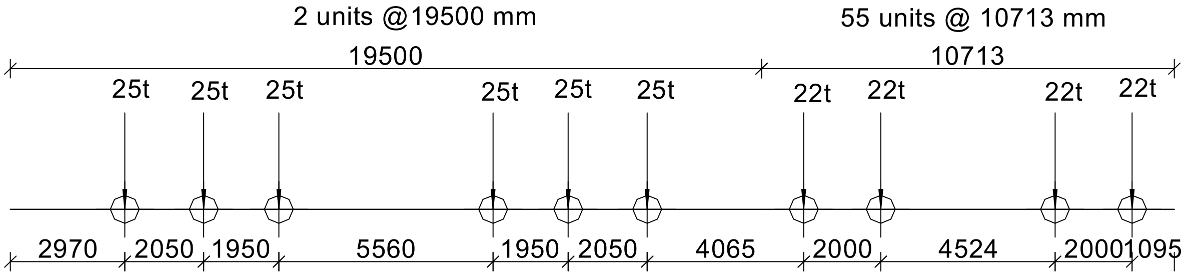

(j) MBG-L

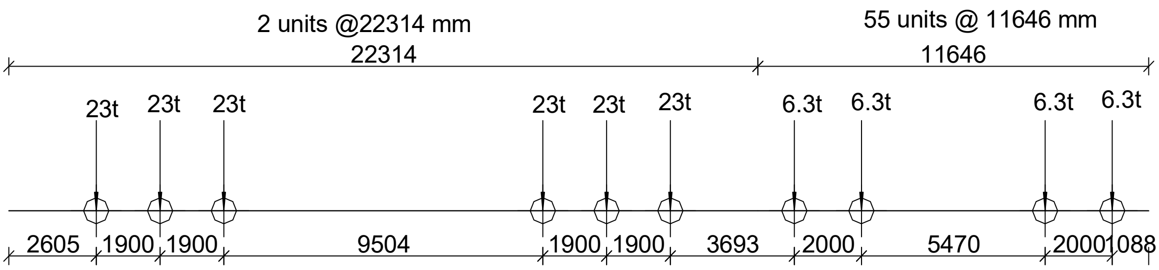

(k) CC+8+2T-E

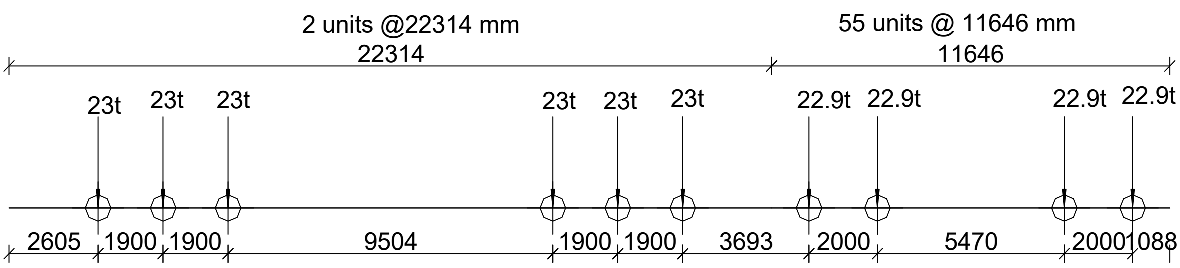

(l) CC+8+2T-L

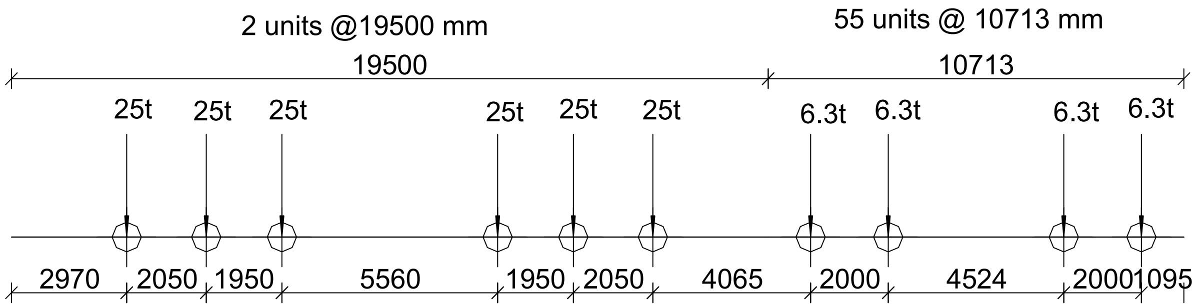

(m) 25T-E

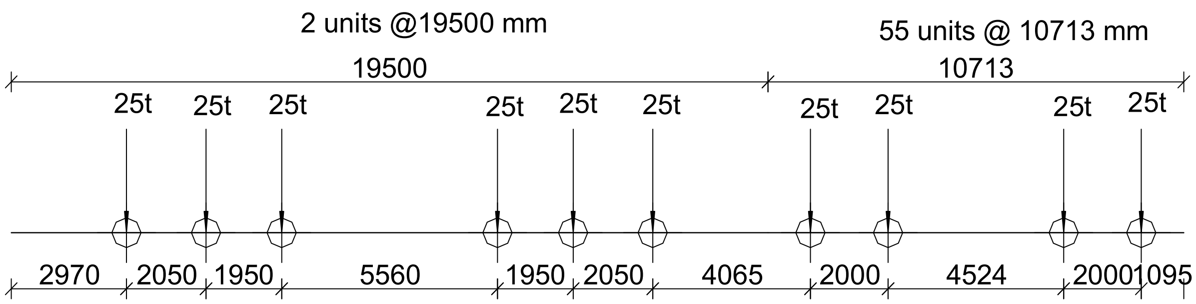

(n) 25T-L

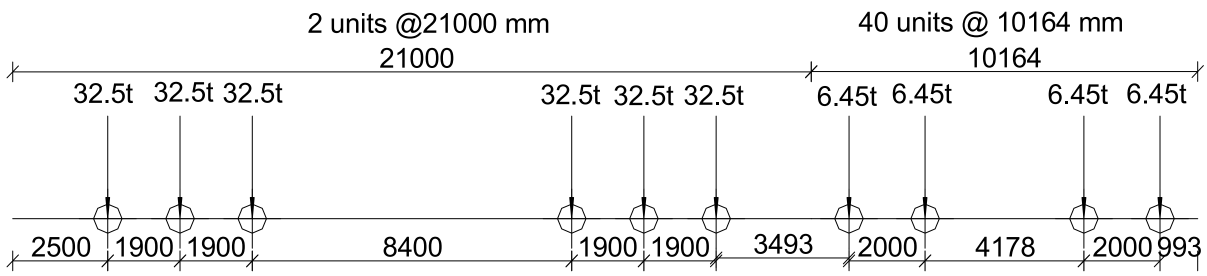

(o) 32.5T-E

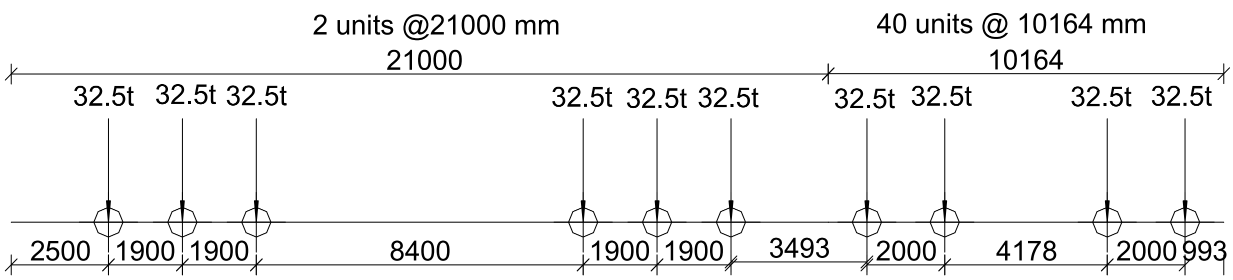

(p) 32.5T-L

Figure 4.3: Loading over the bridge as per bridge rules (RDSO 2014)

[Note-axle loads are in tonne and linear dimensions are in mm]

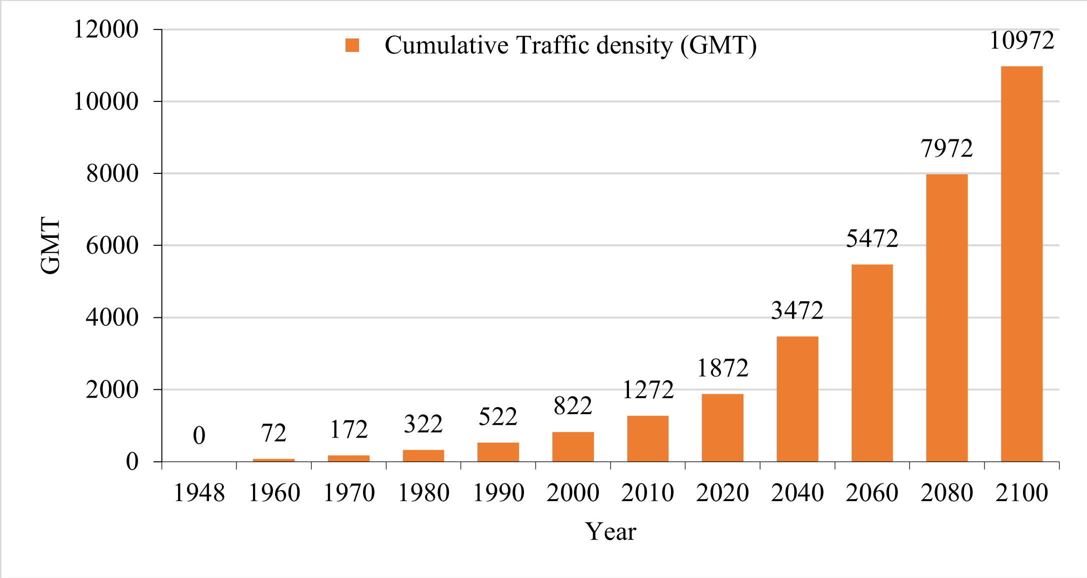

Figure 4.4: Cumulative traffic density over the years

Table 4.1(a) provides nomenclature and details of various types of trains used in herein study. Per vehicle passage damage (PVPD) for each type of train provided in Table 4.1(a) is calculated. Table 4.1(b) lists various past and future loadings, GMT per track, and per day train combination corresponding to GMT. The rate of increase of traffic will be higher in the future in comparison to the past, same has been adopted in future forecasting of rail traffic. All past and future loading mentioned in the Table 4.1(b) are used for calculating fatigue damage and hence remaining life of bridge due to combination of trains passing through the rail cum road bridge since re-girdering of the bridge. For all three futuristic loadings passenger trains, PT-22 and PT-26 are the same, only freight trains vary. Same number of trains in combination are used for all three future loading as the GMT of all loaded freight trains (CC+8+2T-L, 25T-L. 32.5T-L) are not having much difference, and GMT of all empty freight trains (CC+8+2T-E, 25T-E, and 32.5T-E) are almost same Table 4.1(a). Due to speed caution, trains run at speed less than 50kmph over the bridge currently. But bridge is analyzed for three different speed criteria to fulfil future requirements. The nomenclature of future loadings types, Speed cases, and Stress bands is presented in in Table 4.3.

Table 4.1(a): Nomenclature and details of various type of trains

S. No.	Train name	Combination (Locomotive + coach or wagon)	GMT per train	Length (m)	No. of load generated in STAAD
1	PT-EMU	3(LC)+9 coach	0.269	254.26	500
2	PT-22	2(LC)+22ICF coach	0.510	524.25	500
3	PT-26	2(LC)+26ICF-AC coach	0.726	613.44	700
4	BGML-E	2(LC)+55BOXN wagon	0.610	634.30	700
5	BGML-L	2(LC)+55BOXN wagon	1.792	634.30	700
6	RBG-E	2(LC)+55BOXN wagon	0.610	634.00	700
7	RBG-L	2(LC)+55BOXN wagon	1.778	634.00	700
8	MBG-E	2(LC)+55BOXN wagon	0.610	624.15	700
9	MBG-L	2(LC)+55BOXN wagon	1.880	624.15	700
10	CC+8+2T-E	2(LC) + 55BOXN wagon	0.610	681.47	700
11	CC+8+2T-L	2(LC) + 55BOXN wagon	1.948	681.47	700
12	25T-E	2(LC) + 55BOXN wagon	0.610	624.15	700
13	25T-L	2(LC) + 55BOXN wagon	2.120	624.15	700
14	32.5T-E	2(LC) + 55Gondala wagon	0.610	588.53	700
15	32.5T-L	2(LC) + 40Gondala wagon	2.070	445.07	700

Note: where E- empty freight train, L- loaded freight train, PT- passenger train, EMU-electric multiple unit, LC- locomotive, BGML- broad gauge main line, RBG- revised broad gauge, MBG- modified broad gauge, CC- carrying capacity, T-tons, GMT: gross million tons, it is the total train load per year.

Table 4.1(b): Loadings and train combinations

Traffic type	Railway loading	Year	Traffic density per track (GMT)	Train combination per day
Past traffic (before year 2020)	BGML loading	1948-1960	6	5x(PT-EMU) + 2x(BGML-E) + 2x(BGML-L)
	BGML loading	1960-1970	10	10x(PT-EMU) + 3x(BGML-E) + 3x(BGML-L)
	BGML loading	1970-1980	15	12x(PT-EMU) + 5x(BGML-E) + 5x(BGML-L)
	RBG loading	1980-1990	20	10x(PT-EMU) + 6x(PT-22) + 6x(RBG-E) + 6x(RBG-L)
	RBG loading	1990-2000	30	20x(PT-EMU) + 10x(PT-22) + 8x(RBG-E) + 8x(RBG-L)
	MBG loading	2000-2010	45	20x(PT-EMU) + 20x(PT-22) + 12x(MBG-E) + 12x(MBG-L)
	MBG loading	2010-2020	60	25x(PT-22) + 25x(PT-26) + 12x(MBG-E) + 12x(MBG-L)
Future traffic-1 (After year 2020)	CC+8+2T loading	2020-2040	80	35x(PT-22) + 35x(PT-26) + 15x(CC+8+2T-E) + 15x(CC+8+2T-L)
	CC+8+2T loading	2040-2060	100	40x(PT-22) + 40x(PT-26) + 20x(CC+8+2T-E) + 20x(CC+8+2T-L)
	CC+8+2T loading	2060-2080	125	50x(PT-22) + 50x(PT-26) + 25x(CC+8+2T-E) + 25x(CC+8+2T-L)
	CC+8+2T loading	2080-2100	150	60x(PT-22) + 60x(PT-26) + 30x(CC+8+2T-E) + 30x(CC+8+2T-L)
Future traffic-2 (After	25T loading	2020-2040	80	35x(PT-22) + 35x(PT-26) + 15x(25T-E) + 15x(25T-L)
	25T loading	2040-2060	100	40x(PT-22) + 40x(PT-26) + 20x(25T-E) + 20x(25T-L)

year 2020)	25T loading	2060-2080	125	50x(PT-22) + 50x(PT-26) + 25x(25T-E) + 25x(25T-L)
	25T loading	2080-2100	150	60x(PT-22) + 60x(PT-26) + 30x(25T-E) + 30x(25T-L)
Future traffic-3 (After year 2020)	32.5T loading	2020-2040	80	35x(PT-22) + 35x(PT-26) + 15x(32.5T-E) + 15x(32.5T-L)
	32.5T loading	2040-2060	100	40x(PT-22) + 40x(PT-26) + 20x(32.5T-E) + 20x(32.5T-L)
	32.5T loading	2060-2080	125	50x(PT-22) + 50x(PT-26) + 25x(32.5T-E) + 25x(32.5T-L)
	32.5T loading	2080-2100	150	60x(PT-22) + 60x(PT-26) + 30x(32.5T-E) + 30x(32.5T-L)

Table 4.2: Lab test results of steel samples taken from existing bridge

sample	Width (mm)	Thickness (mm)	Length (mm)	Cross sectional area (mm^2)	Yield strength (MPa)	Ultimate strength (MPa)	Elongation (%)
sample-I	55	10	700	550	374.6	535.1	12.3
sample-II	45	10	700	450	390.8	573.1	13.4
sample-III	70	10	700	700	356.2	525.4	17.7
Mean					373.8	544.5	13.7
Standard deviation					17.3	25.2	1.5
Nominal value					356.6	519.3	12.1

Table 4.3: Nomenclature of future loadings types, Speed cases, and Stress bands

	Future loading			Speed			Stress band			
detail	CC+8+2T loading	25T loading	32.5T loading	Up to 50kmph	Equal to 75 kmph	Equal to 100 kmph	without sorting	5MPa	10MPa	15MPa
Nomen-clature	CC+8+2T	25T	32.5T	V1	V2	V3	SB	SB5	SB10	SB15

4.4 Material characterization

Steel samples from bridge are taken out to test the properties of material. Steel was obtained from site, sample prepared and tested as per code IS:1608 (BIS 2005). Steel samples before testing, during testing over universal testing machine and after testing are illustrated in Figure 4.5. Testing results are presented in Table 4.2. Yield strength and ultimate strength of the material is 356.6 MPa and 519.3 MPa respectively. Nominal percentage elongation of material is 12.1%. Obtained elongation of the material is less than provision of code IS:2062 (BIS 2011). Properties of material obtained from laboratory test are compared with properties given in code IS:2062 (BIS 2011). As per material strength obtained by laboratory testing, it can be said that steel used in the bridge was high tensile steel (HTS) of E350 grade (BIS 2011).

Figure 4.5: Lab-tested steel samples before, during and after the test

4.5 FEM modelling

The experimental evaluation of a major bridge, with overall length greater than one kilometre, utilizing the technique of structural health monitoring (SHM) is a very expensive task. STAAD software was used to numerically simulate the bridge. In STAAD software, the bridge is modeled as a space frame steel structure. All bridge members are built-up steel sections, most of the members are made up of plate and angle sections connected by rivets. The elastic characteristics of the material mass density, Young's modulus, and Poisson's ratio are given as: mass density = 7850 kg/m^3, Young's modulus of elasticity =2x10^5 N/m^2, and Poisson's ratio= 0.3. Beam elements are used to model the single span of each major and Minor span of the bridge. The provision of EUDL in lieu of the real axle load is indicated in the bridge regulation (RDSO 2014), axle loads are applied as concentrated loads for precise analysis.

4.5.1 Minor span

STAAD model consists of 248 beam elements and 134 nodes. For fatigue analysis of existing steel rail cum road bridge, total 10100 load combinations (500 each for PT-EMU and PT-22. 700 each for PT-26, BGML-E, BGML-L, RBG-E, RBG-L, MBG-E, MBG-L, CC+8+2T-E, CC+8+2T-L, 25T-E, 25T-L, 32.5T-E, and 32.5T-L) are generated. In this span, stringers and cross beams at rail level are rigidly connected and top flange of both stringer and cross beams are at same level in the existing structure, so rigid connection is provided in the STAAD model to represent the realistic behaviour. Figure 4.6(a) depicts the real image for Minor span of existing rail-cum-road bridge. Configuration of Minor span is given in Figure 4.6(b). There are 6 panels in the Minor span of the bridge. Each panel measures 5.561m with total span length 33.91m.

Figure 4.6(a): Minor span

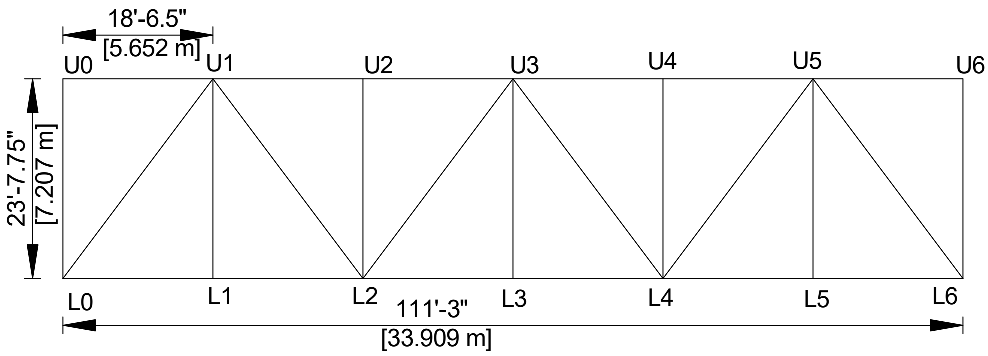

Figure 4.6(b): Configuration of the Minor span members

Figure 4.7(a) depicts three-dimensional STAAD model of the Minor span which has dimensions as per existing span. STAAD model with beam numbers is shown in Figure 4.7(b). Figure 4.7(c) represents the stress diagram obtained due to passage of train 25T-L at rail level and IRC-A vehicle at road level. In Figure 4.8(c), blue colour and red colour indicates tensile stress and compressive stress respectively. Green arrows are representing wheels of the vehicle. Since vehicle load is applied at road and rail level simultaneously in the STAAD model, green arrow can be seen both at road level as well as rail level.

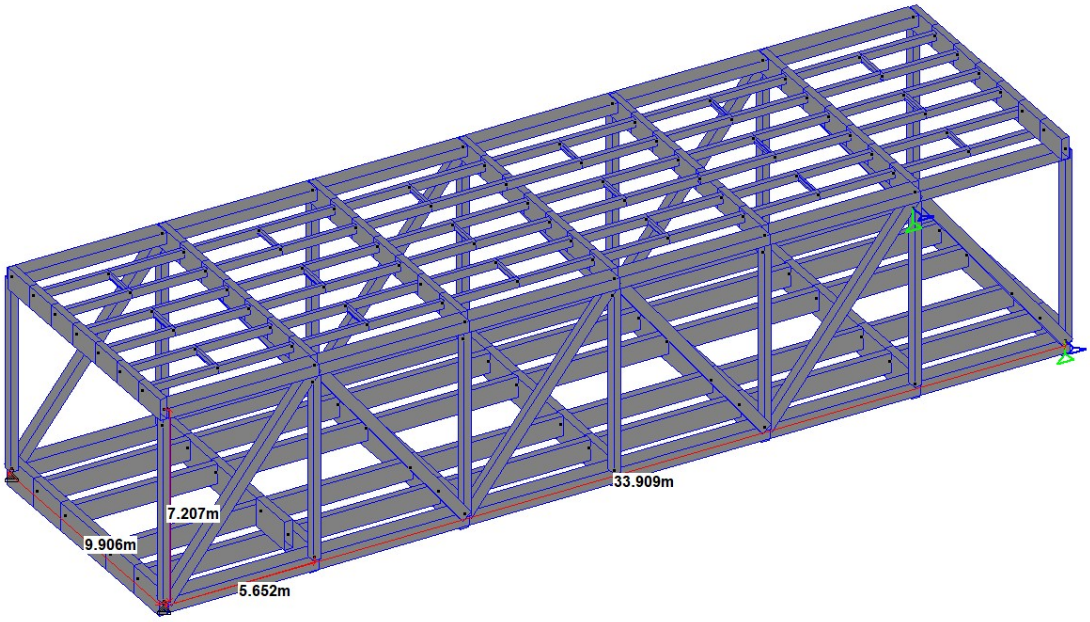

Figure 4.7(a): Three-dimensional STAAD model of the Minor span

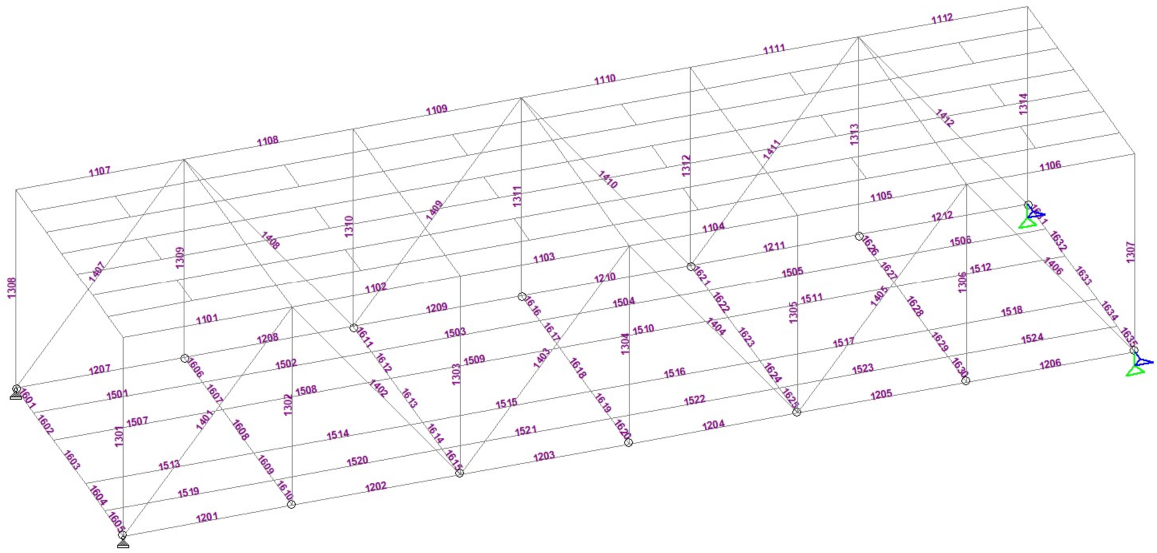

Figure 4.7(b): STAAD model with beam numbers

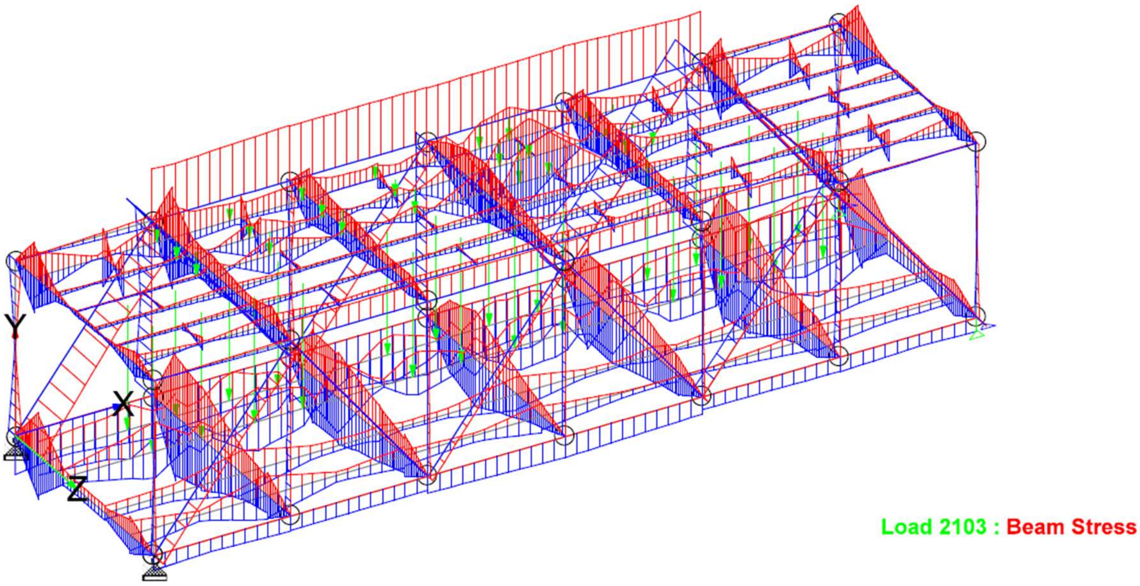

Figure 4.7(c): Stress diagram with train 25T-L at rail level and IRC-A load at road level

4.5.2 Major span

STAAD model consists of 980 beam elements and 553 nodes. For fatigue analysis of existing steel rail cum road bridge, total 10100 load combinations (500 each for PT-EMU and PT-22. 700 each for PT-26, BGML-E, BGML-L, RBG-E, RBG-L, MBG-E, MBG-L, CC+8+2T-E, CC+8+2T-L, 25T-E, 25T-L, 32.5T-E, and 32.5T-L) are generated. In this span stringers are placed above the cross beams at rail level in the existing structure, so hinge connection is provided in the STAAD model to represent the realistic behaviour. Figure 4.8(a) depicts the real image of major span of existing rail-cum-road bridge. Configuration of major span is given in Figure 4.8(b). There are 14 panels in the major span of the bridge. Each panel measures 7.62m with total span length 106.68m.

Figure 4.8(a): Major span

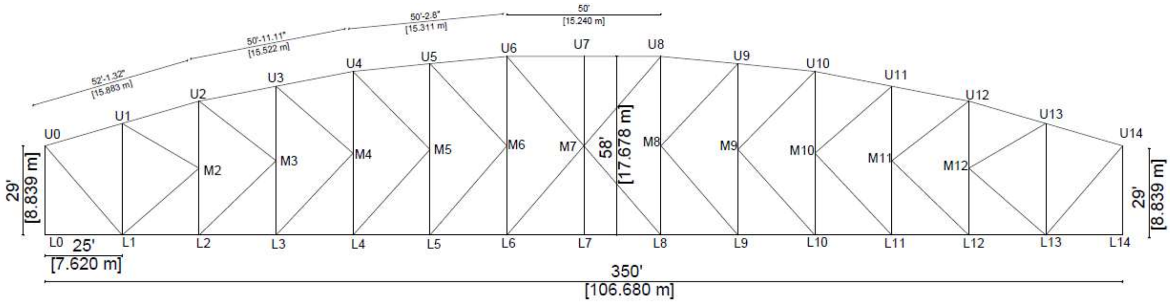

Figure 4.8(b): Configuration of the major span members

Figure 4.9(a) depicts three-dimensional STAAD model of the Major span. STAAD model with beam numbers is shown in Figure 4.9(b). Figure 4.9(c) represents the stress diagram obtained due to passage of train 25T-L at rail level and IRC-A vehicle at road level.

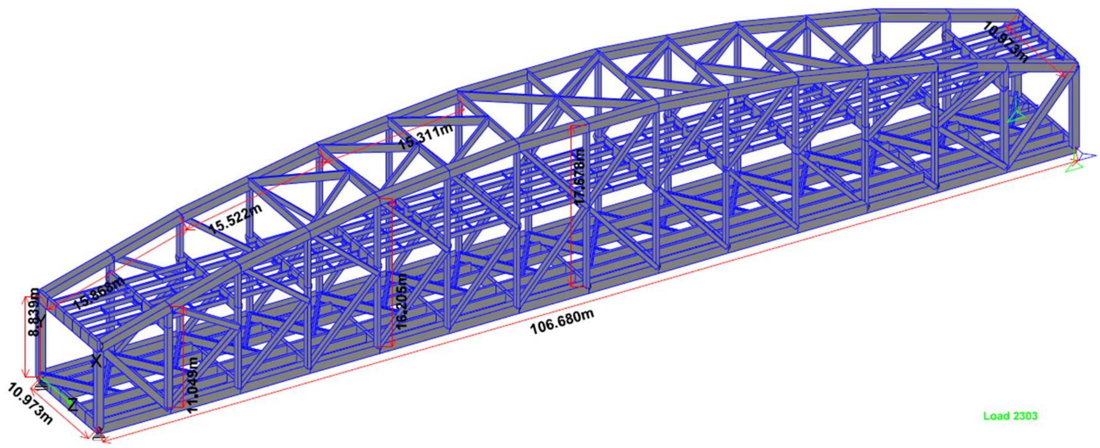

Figure 4.9(a): Three-dimensional STAAD model of the major span

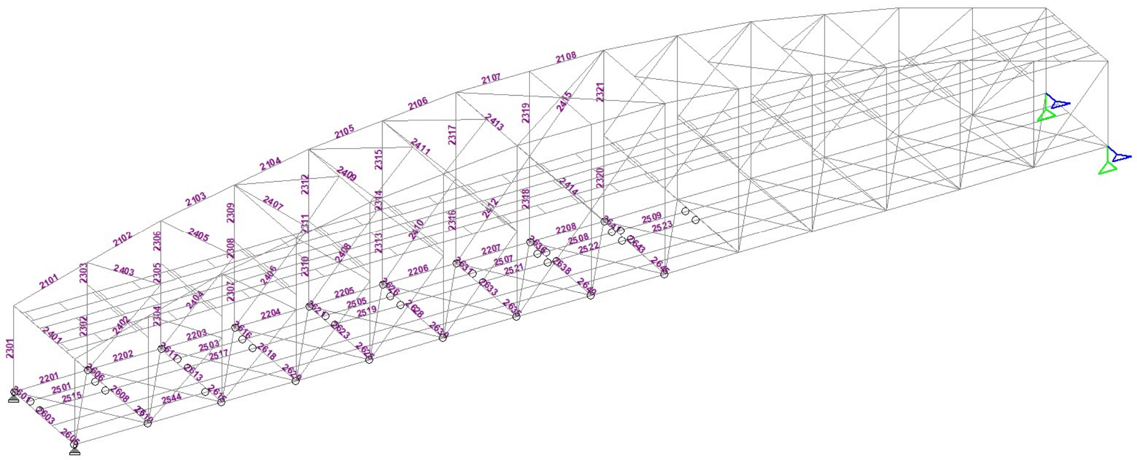

Figure 4.9(b): STAAD model with beam numbers

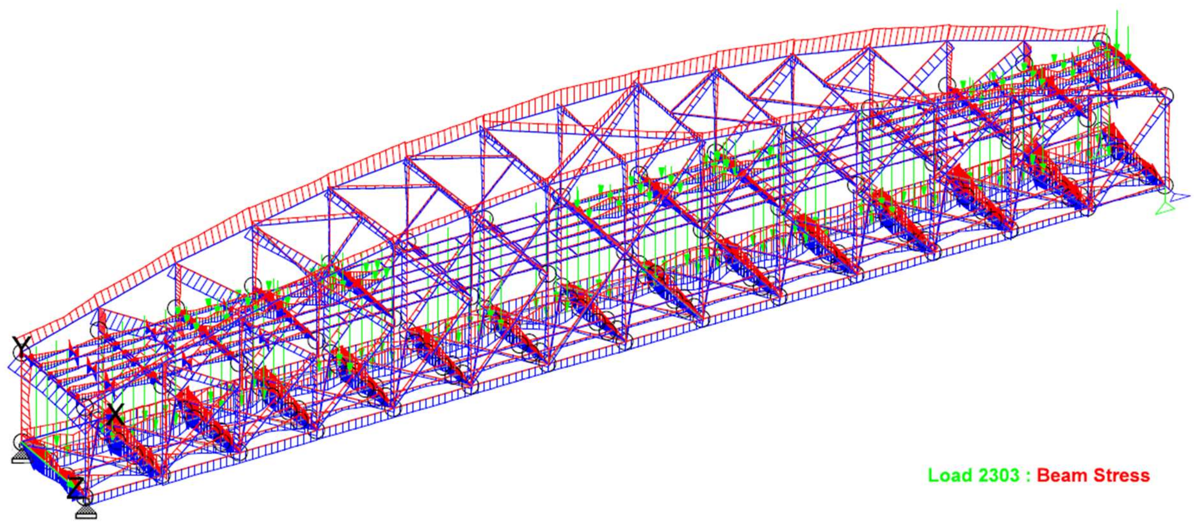

Figure 4.9(c): Stress diagram with train 25T-L at rail level and IRC-A load at road level

4.6 Model validation by deflection check

Due to high cost, continuous monitoring of bridge was not done. FEM model of bridge is validated by deflection measurement at bridge site. Using digital Total Station, deflection is measured at the mid-point of bottom chord of bridge's major span (106.68m). Picture taken during deflection measurement is available with Figure 4.10. At the midpoint (L7) of the bottom chord, the amount of deflection is measured towards both the upline and the downline track. The measured deflection is compared to the calculated deflection from the STAAD model while keeping the load on the STAAD model the same as it was at the moment of deflection measurement on the bridge.

Since only light motor vehicles (LMV) are allowed at road level. During deflection measurement, movement of traffic at road level was not blocked and initial reading was taken when bridge is carrying self-weight as well as weight of vehicles moving at roadway. Final reading was taken when train is also running over railway track. So, deflection at site, which is difference of final and initial reading, is deflection due to train load only. Maintaining same axle load, spacing of axles, and track, deflection due to train is measured by STAAD. Comparison of deflection value obtained from STAAD with those obtained from Total Station is provided in Table 4.4. In all cases deflection is measure at mid-point of bottom chord of the steel truss.

Figure 4.10: Deflection measurement with a digital total station (TS) at the bridge site

Table 4.4: Comparison of deflection measured at site and that obtained by FEM Model [Major span]

Case	Initial reading (m)	Train type	Final reading (m)	Deflection (mm) at site	deflection (mm) by STAAD	% error
1	107.8180	Loaded- freight	107.7951	22.9	23.95	4.58
2	108.1390	Loaded- freight	108.0948	44.2	48.7	10.18
3	104.5420	Empty- freight	104.5161	25.9	28.2	8.88
4	104.5210	Empty- freight	104.5079	13.1	14	6.87

Note: In case-1 and case-4, loading and deflection are on opposite side to each other with reference to centre line of bridge at rail level. In case-2 and case-3, loading and deflection are on same side.

4.7 Methodology

There are three different methods generally used for fatigue-based analysis namely stress life (S-N) method, fracture mechanics approach, and strain life method (Ye et al. 2014). Stress life method is suitable for High cycle fatigue (HCF) like in railway bridges; however, strain life method is suitable for low cycle fatigue (LCF) like in aerospace engineering. Fracture mechanics approach is generally applied to predict the propagation life of initial crack.

4.7.1 Stress life method

In this study stress life method has been used to assess the remaining life as discussed below.

As per Miner rule (Miner 1945)

$$D = \sum r_i = \sum \frac{n_i}{N_i} \tag{4.1}$$

Where n_i denotes number of cycles at the i^{th} stress range. N_i indicates cycles to failure for the i^{th} stress range, r_i denotes the cycle ratio, and D represents the amount of damage.

According to Basquin equation (Basquin 1910)

$$\log_{10} N = \log_{10} K - \mathrm{m} \log_{10} \sigma_r$$

$$N{\sigma_r}^m = K \tag{4.2}$$

Where m is the inverse slope of the log/log N curve, N is the number of repetitions necessary to reach failure at the stress range , and is the range of stress or the stress range in any given cycle. Depending on the detail class, empirical constants K and m apply to material. The type of connection utilised in the structure determines the detail class. m has a fixed value for the specific detail class K.

4.7.2 Basic procedure

Various steps of remaining life calculation of a bridge member are as follows:

1. Based on available dimensions and cross sections of members, STAAD model of span is generated and critical members are identified.
2. Stress history of identified critical members is obtained for each type of vehicle (considered train).
3. According to ASTM E1049-85 (ASTM 2017) rainflow count procedure is applied to find stress range and corresponding number of cycles.

4. No. of repetitions to failure (N) corresponding to stress range is obtained from particular category of S-N curve or Basquin equation based on type of connection (riveted or welded) used in the bridge.
5. Per vehicle passage damage (PVPD) is calculated using Palmgren-Miner rule.
6. For each type of vehicle PVPD is calculated using steps (2) to (5).
7. Since train combination for future loading is unknown. Combination of trains running per day over the bridge is generated based on future forecasted GMT over bridge and GMT of trains. PVPD is used to compute damage per day for combinations of trains.
8. Using linear damage rule (LDR), damage per year is calculated.
9. Remaining damage (RD) at the end of each year is calculated to know amount of damage at particular year.
10. When the damage(D) value is equal to 1.0 or the remaining damage (RD) value is equal to 0, the member is assumed to be failed.

4.7.3 Application of different stress bands

The majority of earlier studies directly analyse the bridge's remaining life using the stress band SB10. However, Patel and Pathak (2023) used the stress life approach and two stress bands (5 MPa and 10 MPa) to determine the remaining life of a railway bridge. The reference stress band 'SB' is not used to calculate remaining life in this study either.

In the current study, a total of four stress bands were used, with SB serving as the reference band and SB5, SB10, and SB15 serving as the other three. No sorting is carried out at stress band SB, and the number of cycles to failure is determined from the S-N curve for a specific category given in (BS: 5400 part 10) according to the stress range of each full or half cycle. In the instance of SB5, stress ranges are sorted and grouped at intervals of 5MPa, and the corresponding number of cycles are recorded; the number of cycles to failure is then calculated for the average value of each stress interval using the S-N curve. Similar procedure is applied for SB10 and SB15.

For each stress band, SB5, SB10, and SB15, the probability density function (PDF) of the best-fit distribution and the normal distribution curve are seen. Probability density function (PDF) (f(x)) of normal distribution, generalized logistic distribution, and log-logistic distribution are defined as below (Johnson et al. (1995)):

Normal distribution:

$$f(x) = \frac{e^{-\frac{1}{2} \times (\frac{x-\mu}{\sigma})^2}}{\sigma\sqrt{2\pi}} \quad \text{for} -\infty < x < \infty \tag{4.3}$$

where, σ –standard deviation or scale parameter , μ- average or location parameter

Generalized Logistic Distribution:

$$f(x) = \begin{cases} \dfrac{(1+kz)^{-\left(1+\frac{1}{k}\right)}}{\sigma1 \left[1+(1+kz)^{-\frac{1}{k}}\right]^2} \ ; \ k \neq 0; \ \text{for} \ 1+k\left(\dfrac{x-\mu_1}{\sigma_1}\right) > 0 \\ \dfrac{e^{-z}}{\sigma1(1+e^{-z})^{-2}} \quad ; \quad k = 0; \quad \text{for} \ -\infty < x < \infty \end{cases} \tag{4.4}$$

where, k- shape parameter, σ_1– scale parameter, μ_1- location parameter

Log-logistic Distribution:

$$f(x) = \frac{\alpha}{\beta} \times \left(\frac{x-\gamma}{\beta}\right)^{\alpha-1} \times \left\{1+\left(\frac{x-\gamma}{\beta}\right)^{\alpha}\right\}^{-2} ; \gamma < x < \infty \tag{4.5}$$

where, α- shape parameter, β- scale parameter, γ – location parameter

In the herein study x is random variable representing variation (%) of different stress bands concerning stress band ‘SB’.

4.8 Result and Discussion

Both minor and major span of the bridge are analysed using stress-life method considering three proposed or future loading (CC+8+2 loading, 25T loading and 32.5T loading), three different speed criteria (V1, V2 and V3) and at four types of stress band (SB, SB5, SB10, and SB15). Meaning of words used in parenthesis is provided in Table 4.3. Actual vehicle load running over the bridge is applied in STAAD model to obtain stress history. Load is applied since re-girdering of the bridge. Initially, PVPD and remaining life have been calculated using stress bands SB, SB5, SB10, and SB15. The variance in PVPD and remaining life for SB5, SB10, and SB15 with respect to stress band SB is investigated. For each stress band, SB5, SB10, and SB15, the probability density function (PDF) of the best-fit distribution and the normal distribution curve are seen. Plotted are two distribution curves: the best-fit curve and the normal distribution curve. Random data typically comes with a normal distribution; in this case, the normal distribution curve is presented alongside the best-fit distribution for comparison.

4.8.1 Minor span

4.8.1.1 Per vehicle passage damage (PVPD)

Analysis of existing rail-cum-road bridge has been done using STAAD. Stress history of X-beam (1618) at midsection due to various trains running at speed V2 is illustrated in Figure 4.11(a). Horizontal axis is representing load steps. All passenger train types, with the exception of PT-EMU, and empty freight train 25T-E experience increasing stress as the locomotive enters the bridge, uniform fluctuation during the passage of waggons or coaches, and decreasing stress as the last coach or wagon exits the span. According to axle load and spacing, stress varies continuously in the case of passenger trains (PT-EMU). With regard to passenger trains (PT-22 and PT-26), stress is quickly lowered when the locomotive passes over the span, and then uniform fluctuation is shown during the passage of the coaches, with the lower limit being close to zero because of the greater distance between the axles of the coaches. All loaded freight trains, including the BGML-L, RBG-L, MBG-L, CC+8+2T-L, 25T-L, and 32.5T-L, experience an increase in stress as the locomotive approaches the span and a subsequent increase in magnitude as the wagons pass through the span. Stress immediately decreased as the locomotive passed through the span in the case of the empty goods train (25T-E), and it stayed nearly constant during the passage of the wagons. Rainflow counting algorithm (ASTM 2017) is applied to obtain stress histogram from stress history.

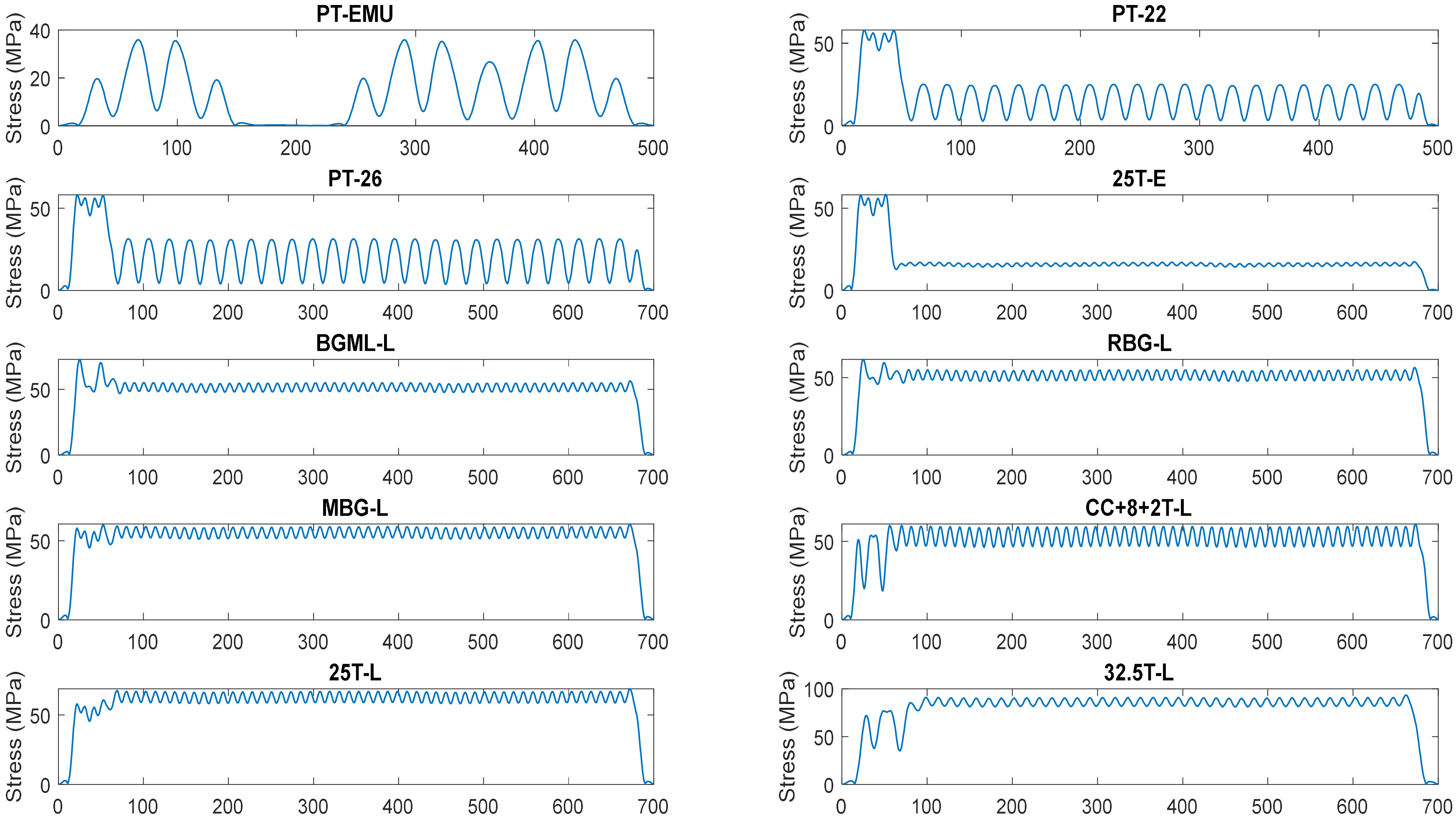

Figure 4.11(a): Stress history of the X-beam (1618) at midsection due to various trains running at speed v2 [Minor span] (Note-In the x-axis, values represent load steps)

Figure 4.11(b) illustrates three dimensional rainflow matrix histogram and the stress history of diagonal (L2U3,1409) obtained with the help of MATLAB due to PT-22 train running over the span at speed V1. The top portion of the graphic displays the stress history, and the bottom portion displays the stress histogram that is generated using the rainflow algorithm.

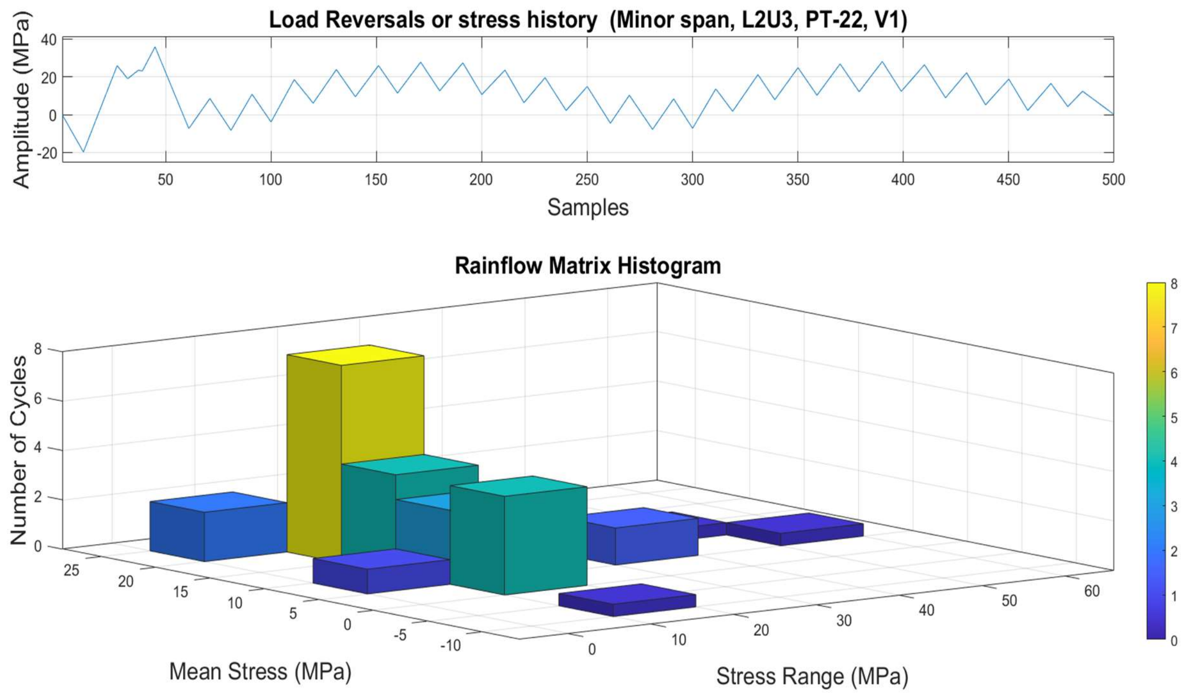

Figure 4.11(b): 3D rainflow matrix histogram with stress history of diagonal (L2U3, 1409) due to train: PT-22 [Minor span]

4.8.1.2 Remaining life

The members that are either subjected to tensile stress or stress reversal and exhibit more stress fluctuation than other members are considered critical members. Members that are merely continuously subjected to compressive stress from vehicle passing are not considered critical for fatigue criteria (BSI 1980). Each type (bottom chord, vertical, diagonals, stringer, and cross beam) is chosen to include at least one critical member, with the exception of the top chord, which is always in compression owing to vehicle traffic. Members of the bridge are listed in Table 4.5(b) according to their remaining lives, which are listed in ascending order. Table 4.5(b) provides remaining lives of members considering three futuristic loading, three different speeds, and four stress range intervals.

Table 4.5(a): Identified critical members [Minor span]

Stringer	X-beam	X-beam	X-beam	Bottom chord	Vertical	Diagonal	Diagonal
Stringer, (1504) at end section	X-beam (1616) at mid-section	X-beam (1618) at mid-section	X-beam (1619) at end section	L2L3 (1209)	L3U3 (1311)	L2U3 (1409)	L2U1 (1408)

Table 4.5(b): Remaining life of members [Minor span]

Variables			**Member**							
Future loading	**Speed**	**Stress band**	Stringer (1504) at end	X-beam (1618) at mid	L2U3 (1409)	L2U1 (1408)	L2L3 (1209)	L3U3 1311	X-beam (1619) at end	X-beam (1616) at mid
CC+8+2T	V1	SB	60.5	78.1	87.2	98.1	119.0	265.5	282.0	406.2
		SB5	62.7	80.3	85.5	97.4	123.8	268.1	271.9	413.5
		SB10	58.5	69.1	86.4	99.5	107.7	221.4	239.0	334.2
		SB15	50.7	72.2	84.9	103.4	115.8	254.1	292.5	718.3
	V2	SB	39.7	54.5	63.4	70.5	84.7	184.8	193.7	278.7
		SB5	38.0	52.0	63.8	67.8	83.6	173.3	172.8	266.6

		SB10	34.4	53.6	61.6	67.3	77.9	173.0	159.7	180.3
		SB15	28.2	64.5	54.5	63.1	64.2	143.3	147.2	299.3
	V3	SB	28.7	42.4	51.4	57.8	69.2	148.3	155.0	222.9
		SB5	28.1	45.3	51.4	56.3	68.0	146.9	170.3	200.4
		SB10	29.3	43.4	51.5	55.0	70.9	136.4	159.4	178.3
		SB15	25.8	46.2	47.2	62.3	63.2	134.3	143.0	146.7
25T	V1	SB	53.6	79.3	86.5	90.2	108.8	281.4	271.6	454.6
		SB5	54.9	81.6	85.0	91.0	117.3	272.4	263.1	413.3
		SB10	52.4	72.2	86.0	90.5	108.0	235.3	222.3	323.9
		SB15	46.7	69.7	82.1	96.7	99.5	264.0	292.7	655.5
	V2	SB	34.8	55.4	62.6	65.3	78.0	196.2	186.7	311.3
		SB5	33.5	53.6	62.6	63.3	76.8	178.1	169.6	312.8
		SB10	32.4	57.8	60.4	62.7	72.4	180.5	162.2	234.4
		SB15	26.3	67.0	52.6	59.9	64.4	146.1	136.1	313.5
	V3	SB	24.9	43.0	50.7	53.3	64.1	157.4	149.6	248.6
		SB5	24.3	46.4	50.6	51.5	63.3	160.2	160.9	231.2
		SB10	24.8	44.6	49.9	49.2	65.4	164.6	150.5	232.7
		SB15	21.3	47.7	46.3	56.1	57.2	127.2	132.5	149.7
32.5T	V1	SB	40.9	68.2	75.4	69.0	81.4	236.9	222.2	379.3
		SB5	42.2	70.0	75.4	70.6	84.0	228.7	216.6	355.2
		SB10	39.7	62.9	75.4	71.6	75.7	191.8	196.3	277.8
		SB15	34.2	62.3	74.1	73.4	83.5	222.5	241.3	611.6
	V2	SB	25.6	47.1	54.8	50.2	59.9	165.3	153.8	260.9
		SB5	25.3	45.9	54.6	48.0	60.2	152.8	138.9	269.1

		SB10	23.6	47.5	52.0	47.7	55.3	160.9	134.8	210.6
		SB15	20.7	54.1	48.4	45.6	50.6	133.5	118.9	255.7
	V3	SB	18.4	36.9	43.8	40.5	48.8	133.0	123.8	208.9
		SB5	18.0	38.6	44.2	39.4	47.6	135.2	128.5	194.6
		SB10	18.7	37.2	44.8	37.8	48.4	131.8	120.6	189.1
		SB15	16.8	39.4	39.9	41.9	42.9	109.6	116.1	136.4

Figure 4.12(a) illustrates the remaining life of identified critical members of the major span at stress band ‘SB’ due to various future loading and speeds.

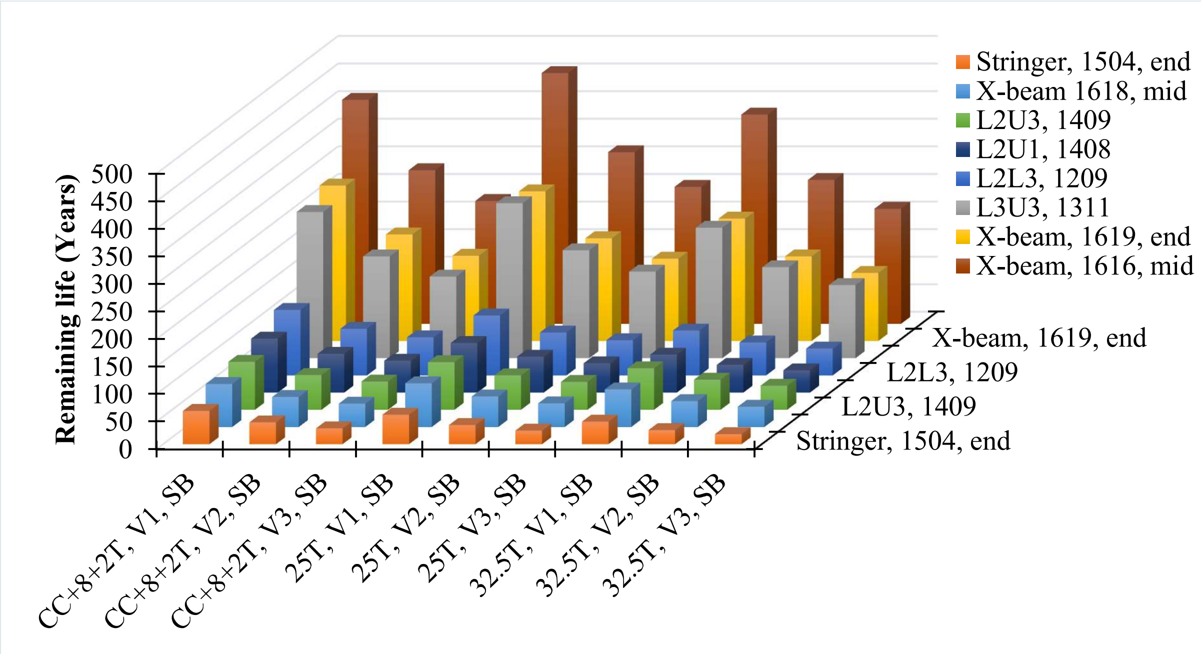

Figure 4.12(a): Remaining life of identified critical members of Minor span at stress band ‘SB’ due to different future loading and speeds [Minor span]

Critical members are those having less remaining life. For the same speed and stress band, the remaining life of bridge members is determined to be minimum, between, and maximum for 32.5T loading, 25T loading, and CC+8+2T loading. Based on the remaining life of bridge members Table 4.5(b), Minor span's three most critical members are stringer (1504) at end, X-beam (1618) at midsection, and diagonal L2U3 (1409) respectively. Figure 4.12(b) compares the remaining life of the three most critical members of the Minor span due to the shift in the stress band for the CC+8+2T loading at speed V1. From this figure, it is clear that the remaining life of the member derived using the various stress bands (SB, SB5, SB10, and SB15) is different for the same loading and speed.

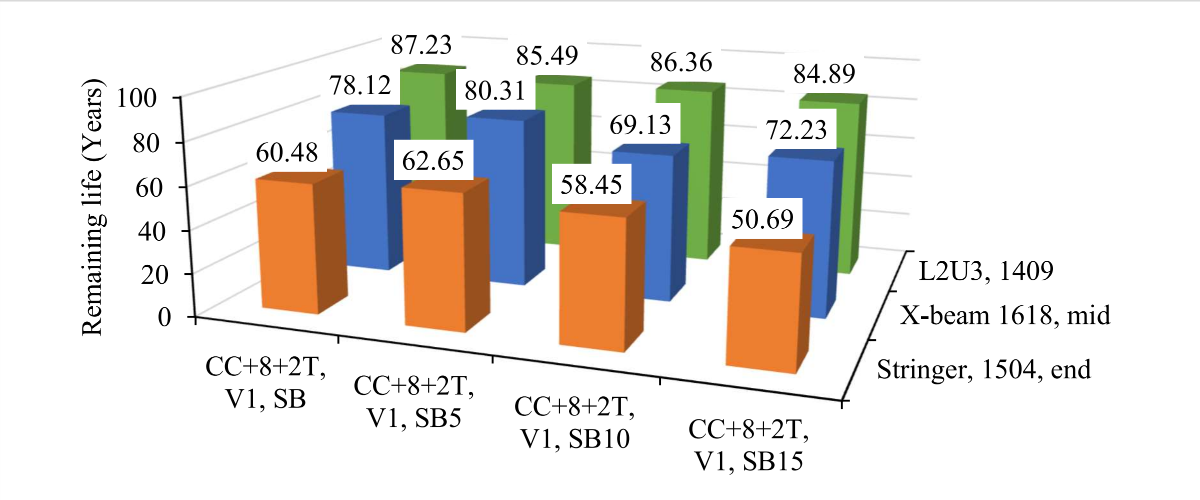

Figure 4.12(b): Comparison of the remaining life of 3 most critical members of Minor span due to change in stress band for CC+8+2T loading at speed V1. [Minor span]

4.8.1.3 Different stress bands

24 datapoints obtained corresponding to 8 identified critical members Table 4.5(a) for three different vehicle speeds (V1, V2, and V3). 24 datapoints are obtained for both PVPD and remaining life at stress band SB, SB5, SB10 & SB15. Figure 4.13(a) illustrates variation in PVPD and remaining life at SB5, SB10, and SB15 concerning 'SB'. In this figure 10-different types of trains are considered for PVPD and 3 different types of loading are undertaken for remaining life. Figure 4.13(b) shows the PVPD variation and remaining life variation histogram, best-fit distribution curve and normal distribution curve. After comparing the goodness-of-fit test results, the best-fit distribution of various distribution curves is chosen.

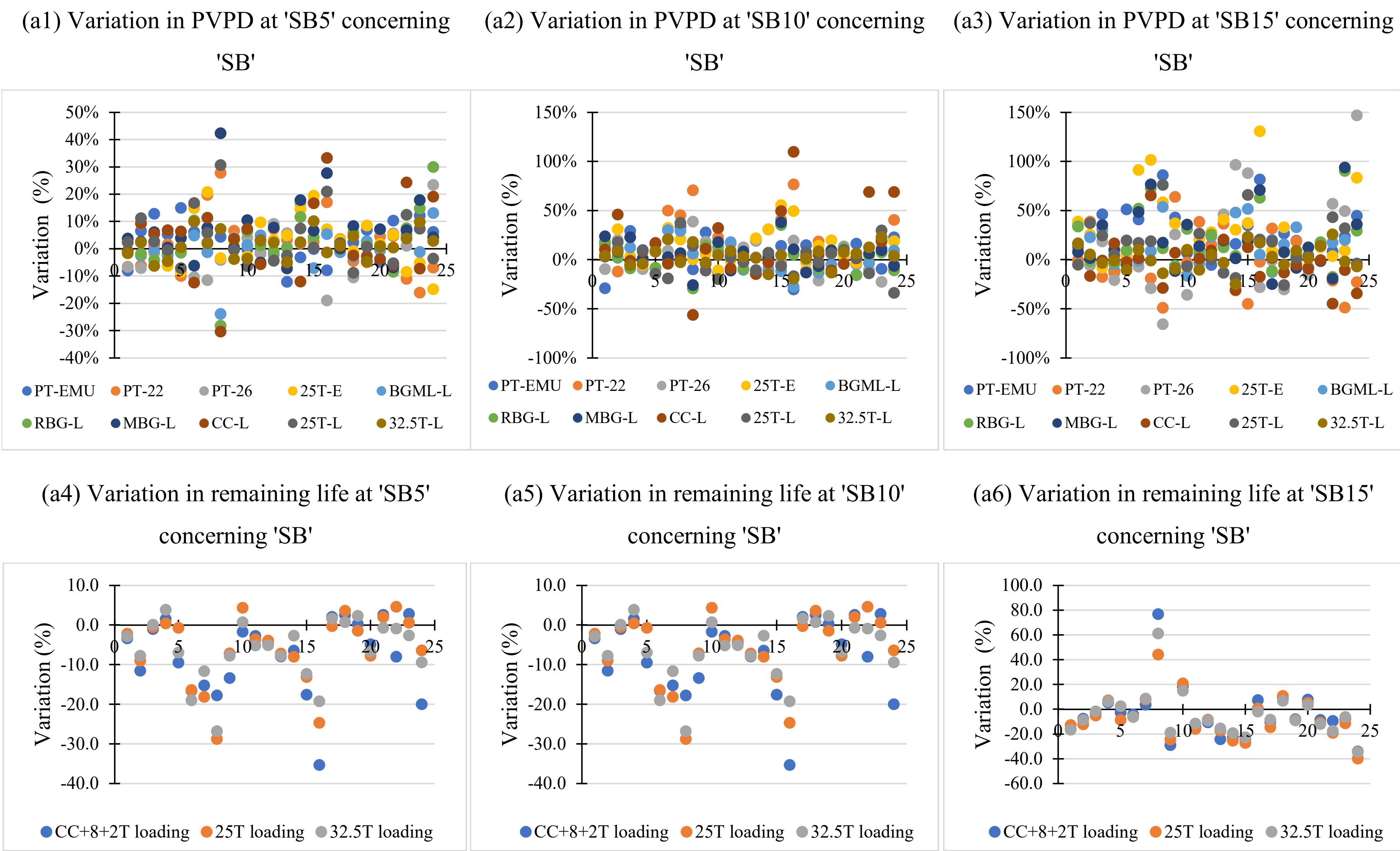

Figure 4.13(a): Variation in PVPD and remaining life regarding stress band ‘SB’ [Minor span]

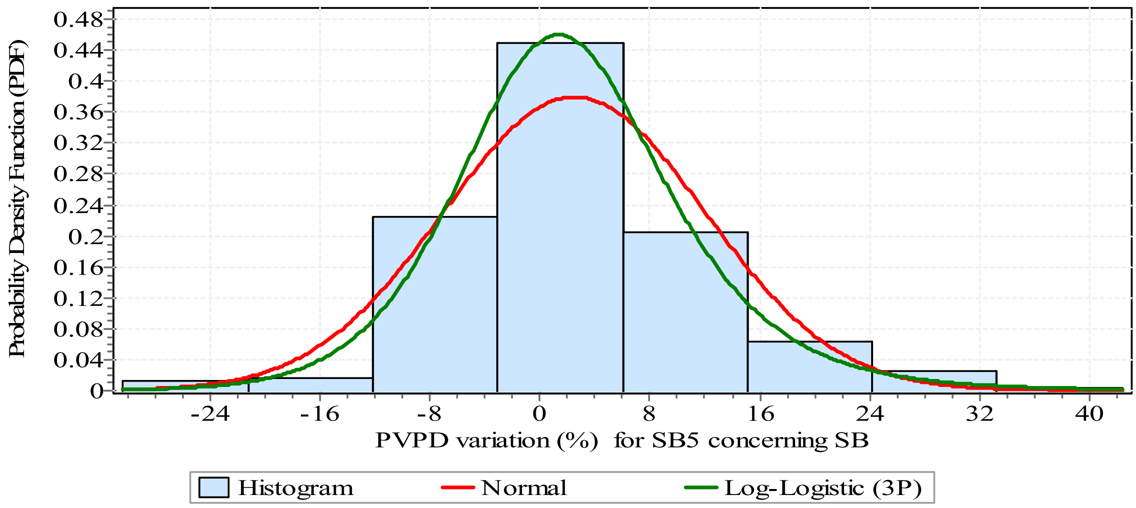

(b1) Variation in PVPD at 'SB5' concerning 'SB'

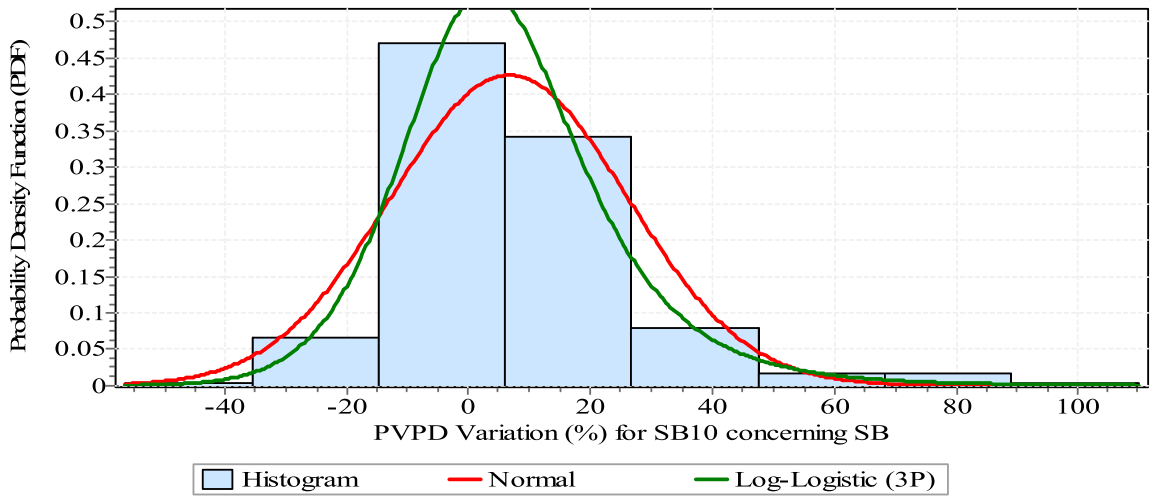

(b2) Variation in PVPD at 'SB10' concerning 'SB'

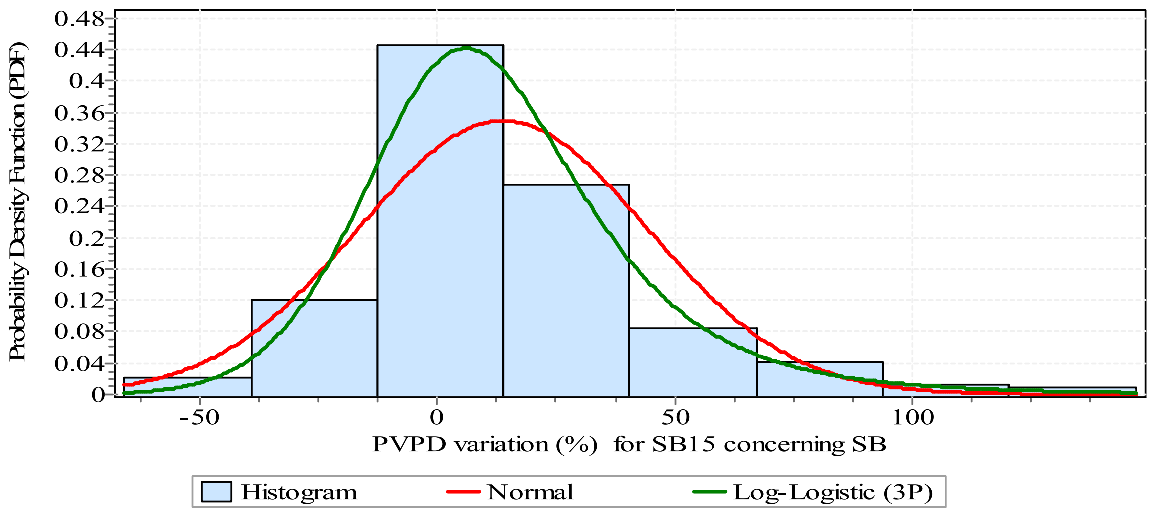

(b3) Variation in PVPD at 'SB15' concerning 'SB'

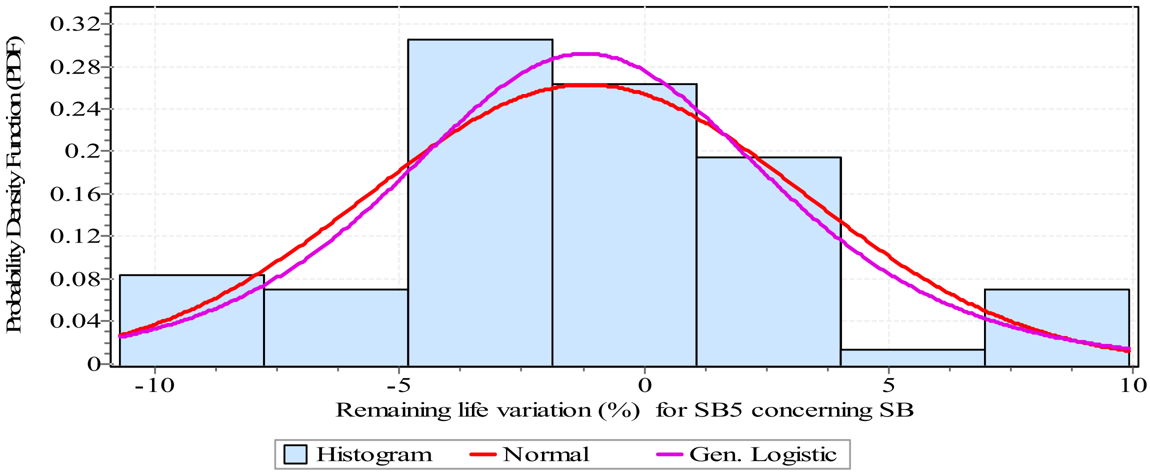

(b4) Variation in remaining life at 'SB5' concerning 'SB'

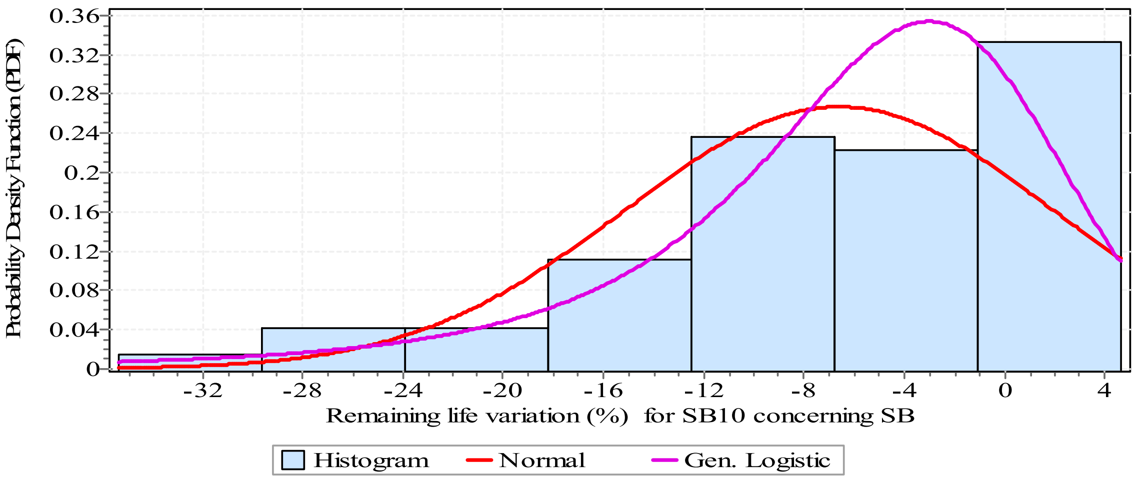

(b5) Variation in remaining life at 'SB10' concerning 'SB'

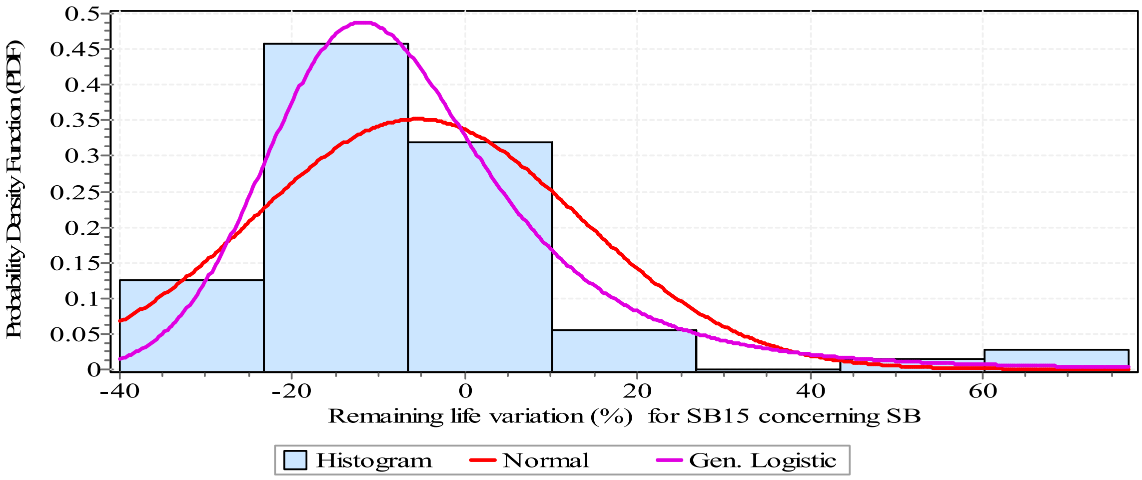

(b6) Variation in remaining life at 'SB15' concerning 'SB'

Figure 4.13(b): PVPD variation and remaining life variation histogram, best fit curve and normal distribution curve. [Minor span]

Table 4.6 provides summary of variation due to different stress bands (SB5, SB10, and SB15) to stress band ('SB') for PVPD and remaining life. Eqn 4.3, 4.4, and 4.5 provide the equation for PDF for general, log-logistic, and generalized logistic distributions respectively. And Table 4.6 provides the parameters of these distributions. For PVPD, concerning stress band 'SB', variation ranges from -30% to 42%, -56% to 110%, and -66% to 147% for SB5, SB10 and SB15 respectively. For remaining life, concerning stress band 'SB', variation ranges from -11% to 10%, -35% to 5%, and -40% to 77% for SB5, SB10 and SB15 respectively.

Table 4.6: Statistical parameters of distributions for variation in PVPD and remaining life concerning stress band 'SB' [Minor span]

Particular	Stress band	Lower limit (%)	Higher limit (%)	Parameters of best-fit distribution (log-logistic)			Parameters of normal distribution	
				(α)	(β)	(γ)	(σ)	(μ)
PVPD	SB5	-30.3	42.3	18.304	90.631	-88.748	9.5435	2.499
PVPD	SB10	-56.2	109.7	10.491	101.11	-96.419	19.393	6.6726
PVPD	SB15	-65.8	146.8	7.7126	118.03	-108.21	30.388	13.751
Particular	Stress band	Lower limit (%)	Higher limit (%)	Parameters of best-fit distribution (generalized-logistic)			Parameters of normal distribution	
				(k)	(σ_1)	(μ_1)	(σ)	(μ)
Remaining life	SB5	-10.7	9.9	0.00401	2.5182	-1.1847	4.4678	-1.1681
Remaining life	SB10	-35.3	4.6	-0.22910	4.2445	-4.9024	8.5168	-6.6042
Remaining life	SB15	-39.8	76.8	0.19493	8.8603	-8.4482	18.881	-5.4778

From Table 4.5(b), most critical member of the Minor span is stringer (1504). It may last up to 60.5 years if proposed future loading CC+8+2T run over the bridge at speed V1 with anticipated GMT and train combination per day Figure 1(b). But same member may fail within 18.4 years if future loading 32.5T is decided to move at speed V3.

4.8.2 Major span

4.8.2.1 Per vehicle passage damage (PVPD)

Analysis of existing railway bridge has been done using STAAD. Stress history of X-beam (2638) at midsection due to various trains running at speed V2 is illustrated in Figure 4.14(a). Horizontal axis is representing load steps. The pattern of stress history fluctuation brought on by different trains crossing the bridge's major span is similar to that of the bridge's Minor span.

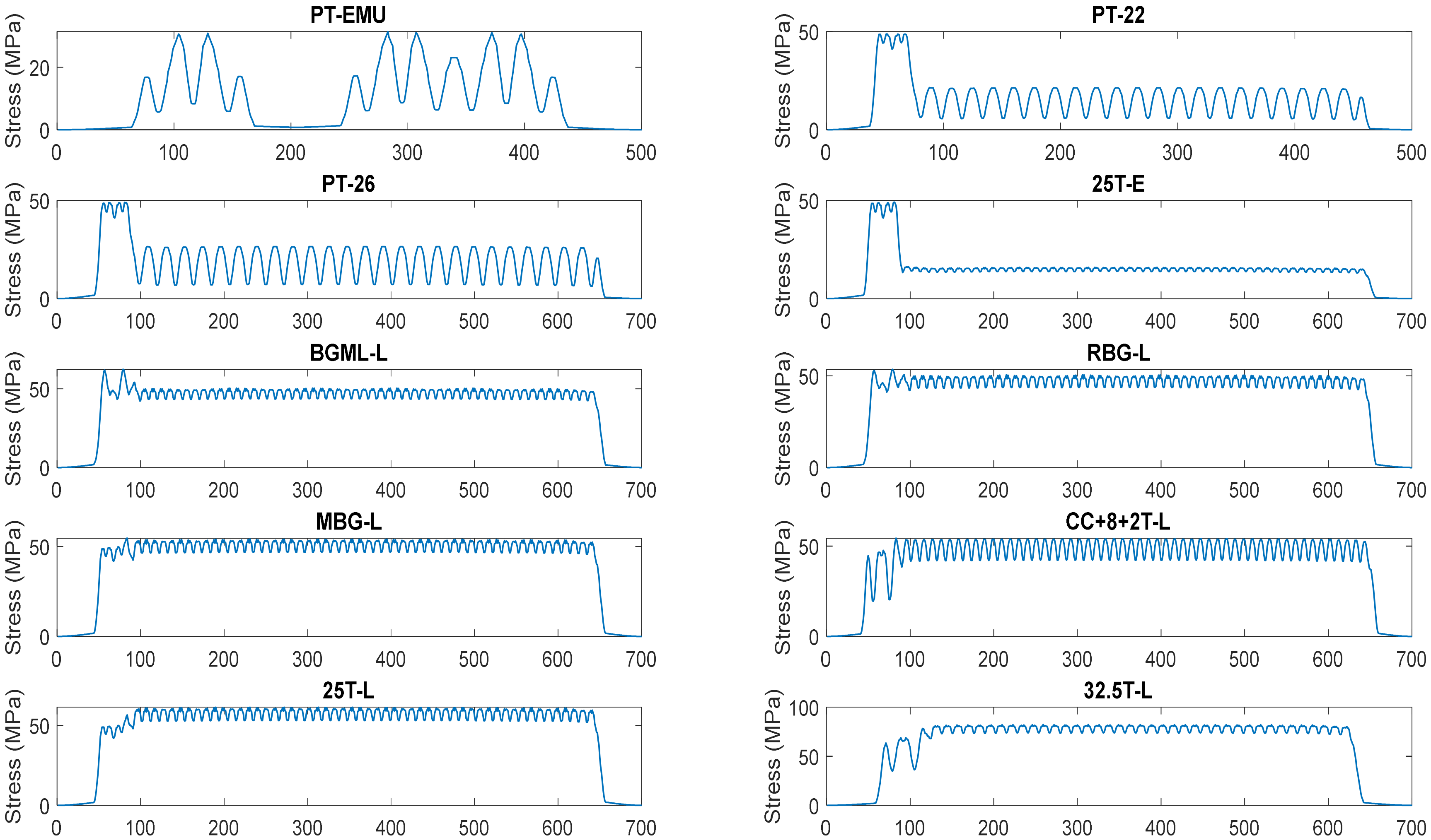

Figure 4.14(a): Stress history of X-beam (2638) at midsection due to various trains running at speed v2 [Major span]
(Note-In the x-axis, values represent load steps)

Rainflow counting algorithm (ASTM 2017) is applied to obtain stress histogram from stress history. Figure 4.14(b) shows three dimensional rainflow matrix histogram and the stress history of diagonal (L6M7,2412) obtained with the help of MATLAB due to passage of train 25T-L.

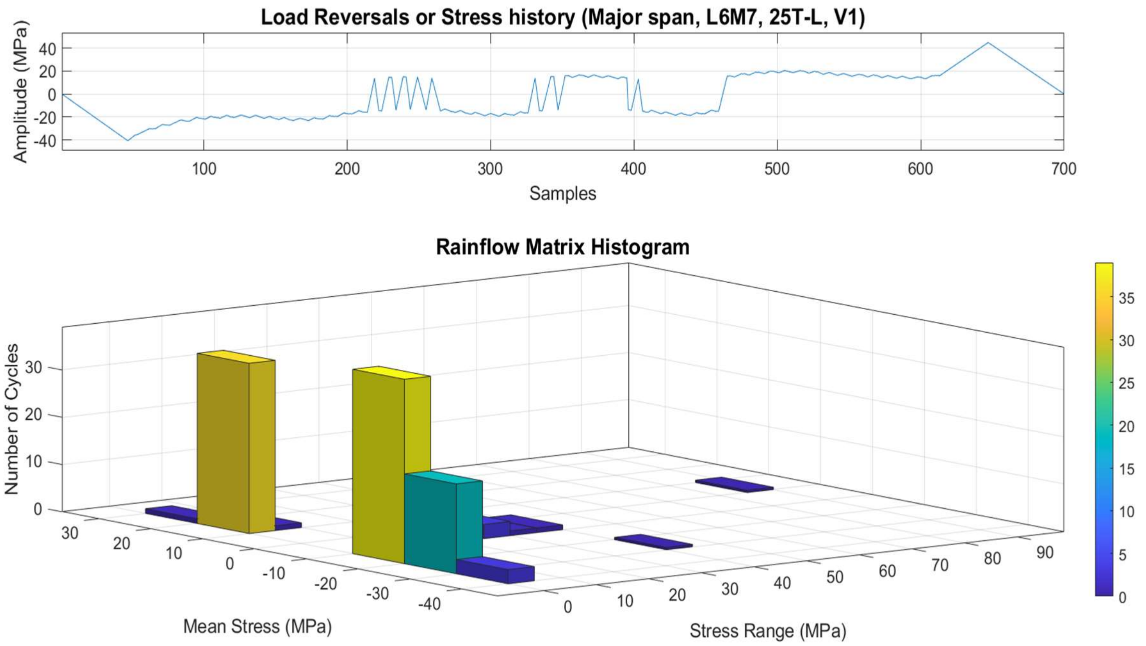

Figure 4.14(b): 3D rainflow matrix histogram with the stress history of diagonal (L6M7,2412) due to train: 25T-L [Major span]

4.8.2.2 Remaining life

Identified critical members of major span are listed in Table 4.7(a). At least one critical member is selected from each type (bottom chord, vertical, diagonals, stringer and cross beam) except top chord as it is always in compression due to plying of vehicles. Table 4.7(b) provides remaining lives of bridge members, members in this table are arranged in ascending order of their remaining lives. For 32.5T loading, 25T loading, and CC+8+2T loading, remaining life of bridge members are obtained minimum, in between and maximum respectively for same speed at stress band SB.

Table 4.7(a): Identified critical members [Major span]

Stringer	X-beam	X-beam	Bottom chord	Vertical	Vertical	Diagonal	Diagonal
stringer (2508) at mid-section	X-beam (2638) at mid-section	X-beam (2638) at end section	L6L7 (2208)	U6M6 (2317)	M2L2 (2304)	U0L1 (2401)	L6M7 (2412)

Table 4.7(b): Remaining life of members [Major span]

Variables			**Member**							
Future loading	**Speed**	**Stress band**	stringer (2508) at mid	L6M7 (2412)	X-beam (2638) at mid	M2L2 (2304)	U0L1 (2401)	L6L7 (2208)	X-beam (2638) at end	U6M6 (2317)
CC+8+2T	V1	SB	65.6	98.1	118.9	124.4	151.8	214.6	273.6	811.0
		SB5	66.3	96.2	121.6	122.3	164.4	197.4	252.0	699.7
		SB10	65.6	91.8	122.1	125.3	155.3	180.6	218.4	638.8
		SB15	59.6	82.4	92.9	121.3	153.3	199.6	302.5	392.6
	V2	SB	42.4	86.6	104.7	110.1	135.7	190.7	240.2	715.1
		SB5	41.4	87.0	108.3	111.6	132.4	195.0	250.4	670.6
		SB10	36.0	80.5	121.2	113.4	129.0	179.8	216.0	621.3
		SB15	35.0	80.9	72.8	96.8	111.7	199.3	302.5	391.1
	V3	SB	33.5	68.4	82.6	87.5	109.9	152.6	188.2	564.0
		SB5	32.7	68.3	79.4	87.7	110.4	149.1	161.4	525.3
		SB10	29.3	66.5	70.2	87.2	113.9	152.0	157.5	560.9
		SB15	30.1	72.0	72.1	81.5	103.2	121.9	132.7	389.5
25T	V1	SB	56.6	89.6	120.9	99.9	122.6	179.7	275.0	687.0
		SB5	55.8	88.1	128.0	98.8	123.7	164.6	244.3	590.3

		SB10	55.3	85.9	143.6	97.0	110.3	153.1	219.6	541.6
		SB15	45.7	80.1	92.9	95.7	114.2	146.0	255.6	338.9
	V2	SB	45.5	78.5	106.5	88.9	109.9	160.0	241.4	605.7
		SB5	44.7	80.2	110.2	87.6	112.0	162.8	242.8	576.3
		SB10	41.9	76.2	130.1	88.8	108.6	152.4	217.1	541.3
		SB15	33.9	74.4	69.0	78.4	90.6	145.8	255.6	337.7
	V3	SB	35.9	61.9	83.9	71.5	89.5	128.7	189.1	477.7
		SB5	34.7	61.0	79.7	71.2	87.9	118.3	158.2	456.2
		SB10	30.7	57.7	72.5	66.8	84.5	127.8	148.9	473.3
		SB15	28.9	59.4	68.3	67.0	85.0	100.9	132.9	336.4
32.5T	V1	SB	37.4	68.2	98.2	60.8	75.4	112.1	215.4	534.8
		SB5	39.0	68.8	103.1	60.3	79.6	103.9	198.2	485.3
		SB10	39.5	67.9	112.9	57.9	79.4	93.4	171.3	456.9
		SB15	36.1	60.4	75.3	62.1	87.0	111.8	195.6	327.2
	V2	SB	33.0	60.9	86.9	54.5	68.2	100.5	189.6	471.9
		SB5	31.9	62.1	89.8	54.8	69.7	103.0	195.7	437.5
		SB10	31.0	58.7	99.5	57.3	67.4	93.0	167.7	391.0
		SB15	31.9	56.8	62.4	48.0	60.4	111.7	195.6	277.1
	V3	SB	26.5	48.1	69.4	43.6	56.7	82.2	149.5	373.2
		SB5	25.3	48.4	67.7	42.9	57.8	80.0	134.0	348.6
		SB10	24.4	44.8	63.0	42.0	55.9	78.6	132.3	376.3
		SB15	27.0	49.4	61.2	41.1	58.0	69.8	116.2	265.9

Remaining life of identified critical members of major span at stress band ‘SB’ due to different future loading and speeds is depicted in Figure 4.15(a).

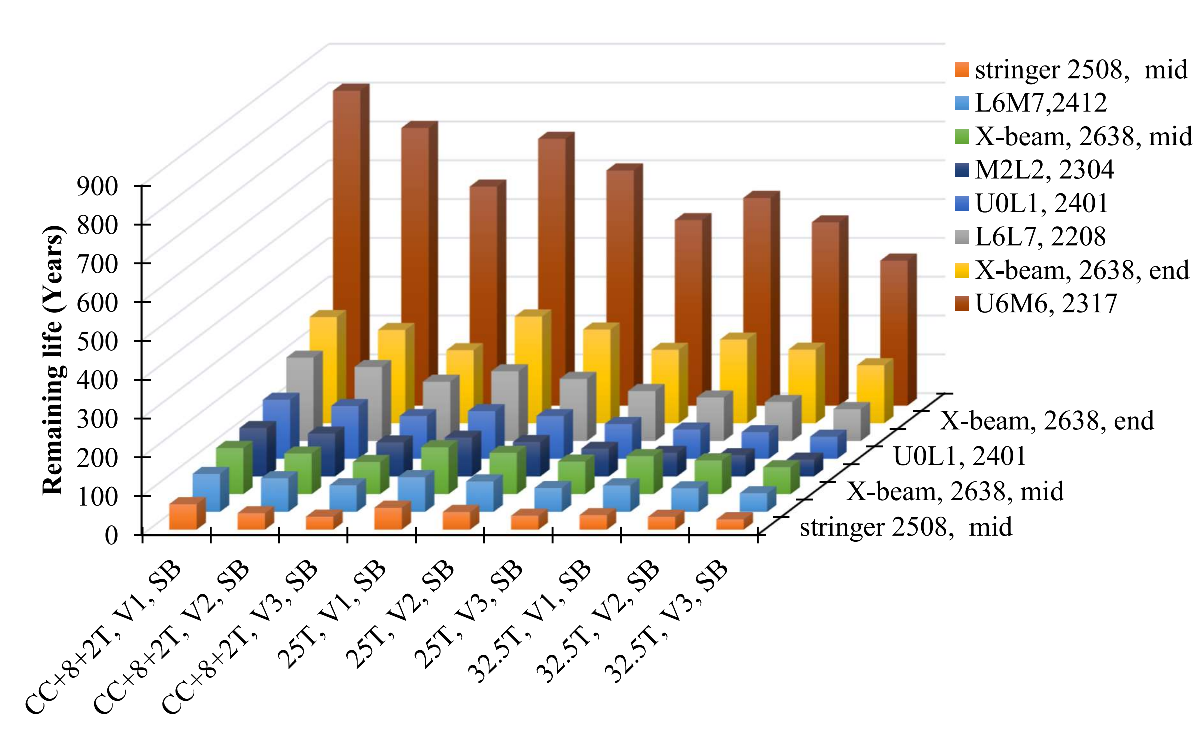

Figure 4.15(a). Remaining life of identified critical members of major span at stress band 'SB' due to different future loading and speeds [Major span]

Based on the remaining life of bridge members Table 4.7(b), major span's three most critical members are stringer (2508) at midsection, diagonal L6M7 (2412), and X-beam (2638) at midsection respectively. Figure 4.15(b) shows comparison of remaining life of 3 most critical members of major span due to change in stress band for CC+8+2T loading at speed V1. From this figure, it can be easily observed that for same loading and speed remaining life of member obtained using different stress band (SB, SB5, SB10, and SB15) is different.

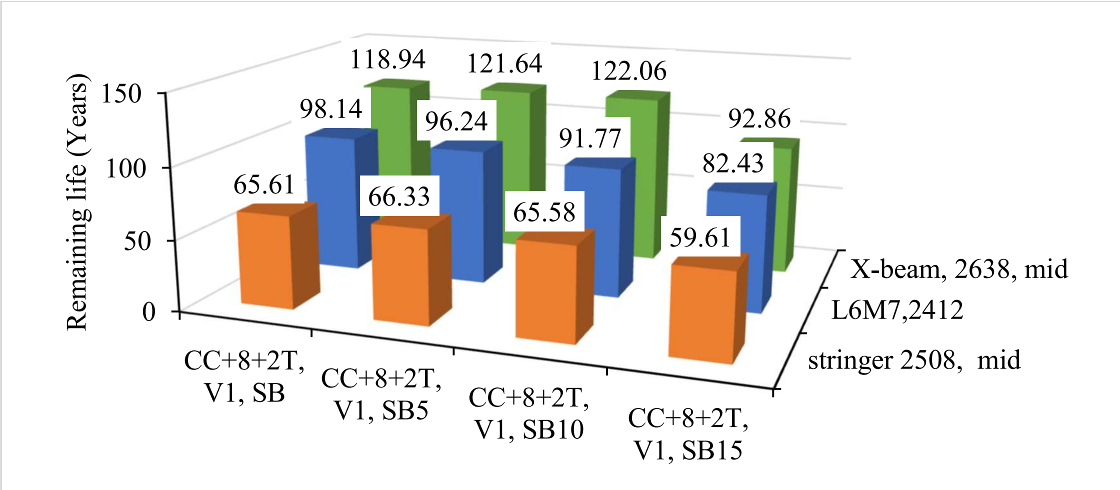

Figure 4.15(b): Comparison of remaining life of 3 most critical members of major span due to change in stress band for CC+8+2T loading at speed V1. [Major span]

4.8.2.3 Different stress bands

Similar to Minor span, 24 datapoint obtained corresponding to 8 identified critical members Table 4.7(a) for three different vehicle speeds (V1, V2, and V3). 24 datapoints are obtained for both PVPD and remaining life at stress band SB, SB5, SB10 & SB15. Figure 4.16(a) illustrates variation in PVPD and remaining life at SB5, SB10, and SB15 concerning 'SB'. In this figure 10 different types of trains are considered for PVPD and 3 different types of loading are undertaken for remaining life. Figure 4.16(b) shows the PVPD variation and remaining life variation histogram, best-fit distribution curve and normal distribution curve. After comparing the goodness-of-fit test results, the best-fit distribution of various distribution curves is chosen.

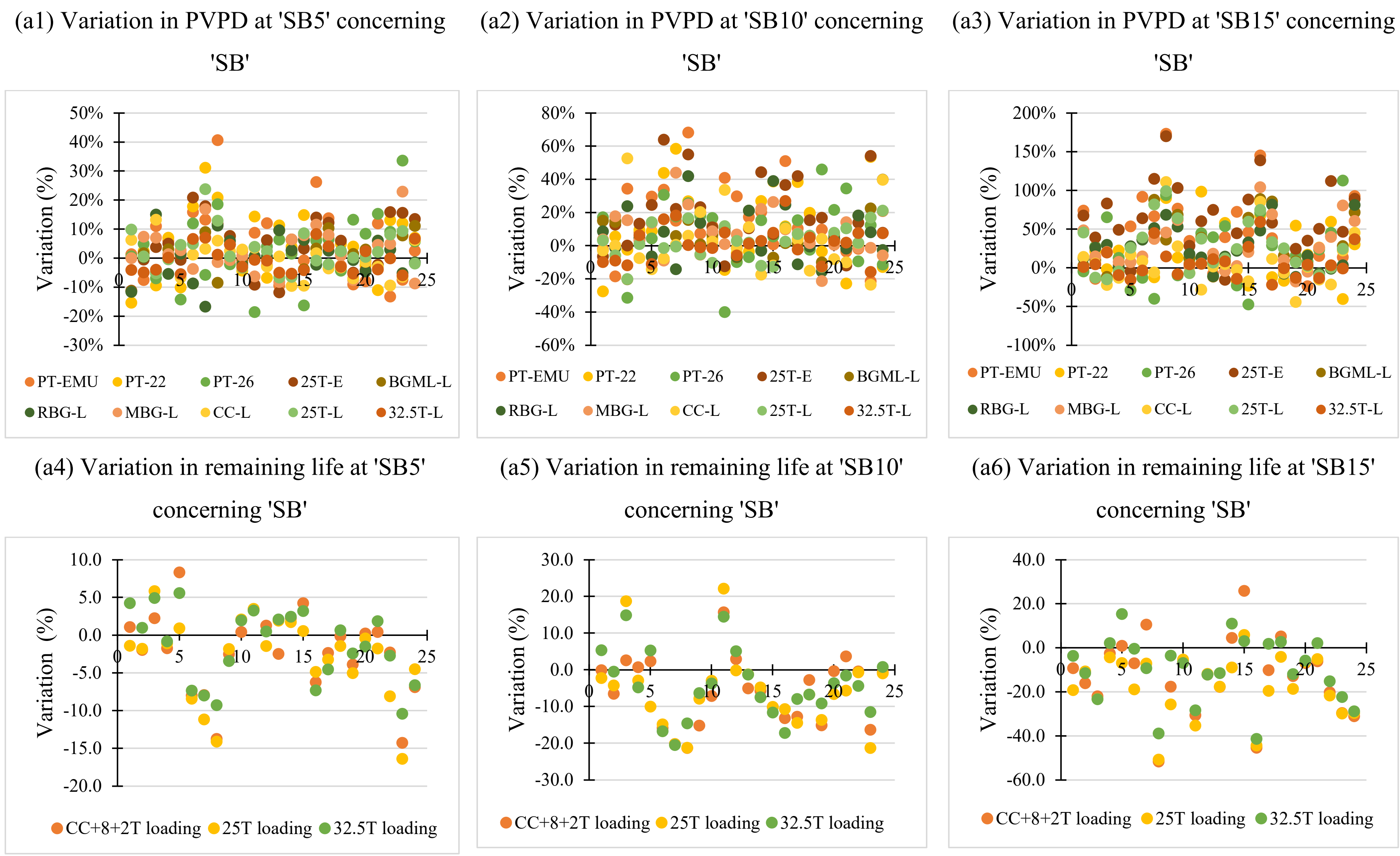

Figure 4.16(a): Variation in PVPD and remaining life regarding stress band ‘SB’ [Major span]

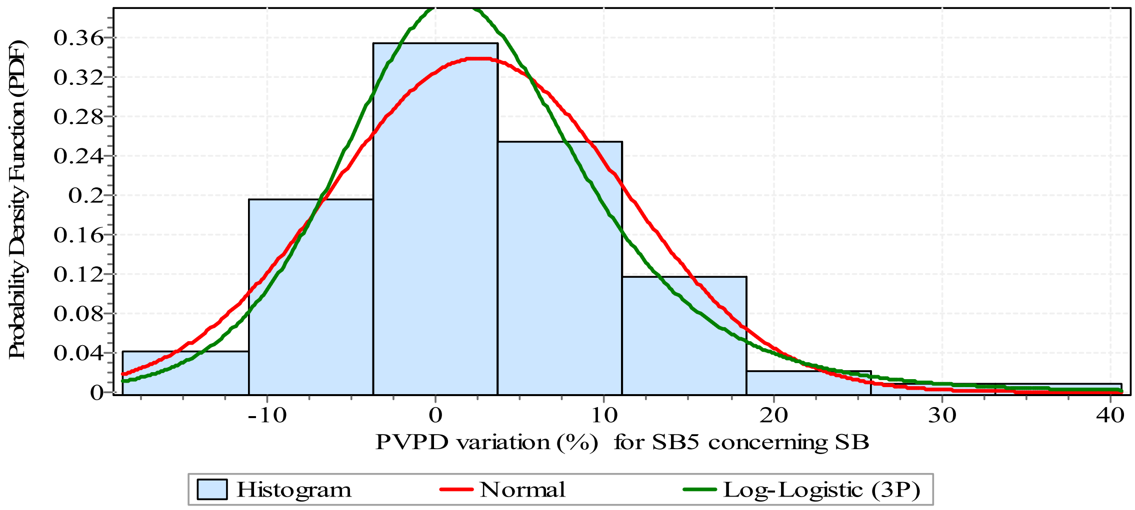

(b1) Variation in PVPD at 'SB5' concerning 'SB'

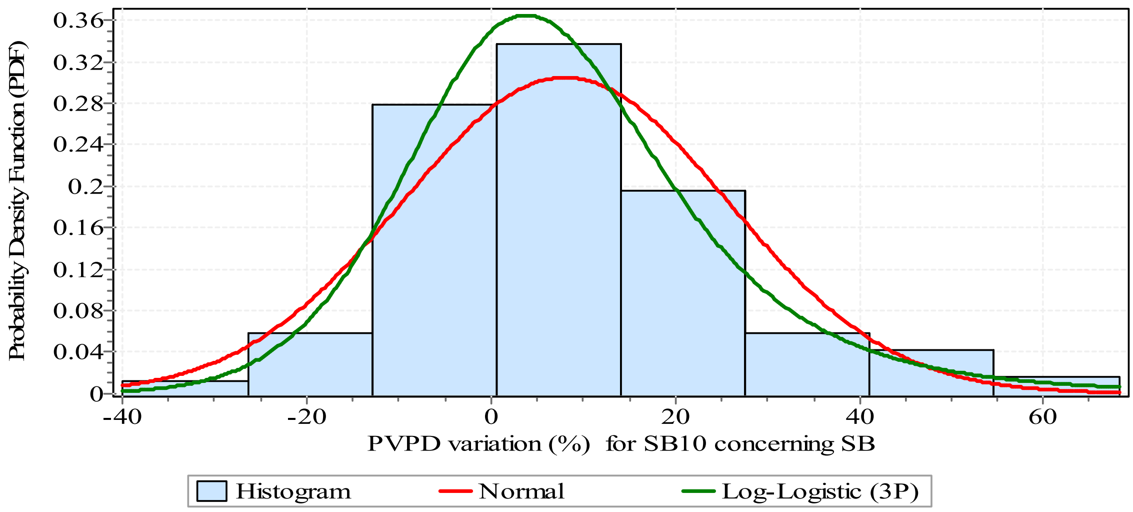

(b2) Variation in PVPD at 'SB10' concerning 'SB'

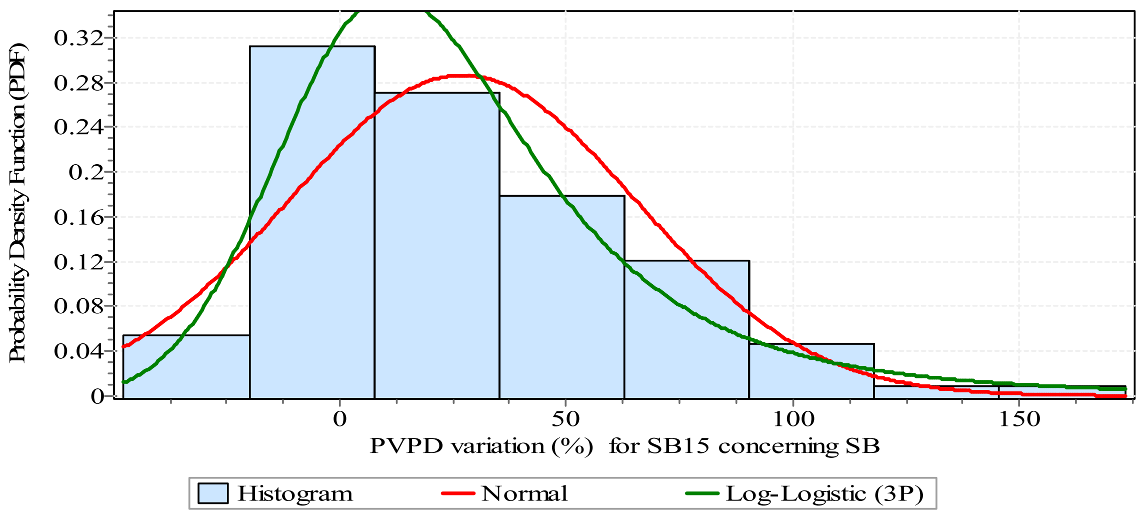

(b3) Variation in PVPD at 'SB15' concerning 'SB'

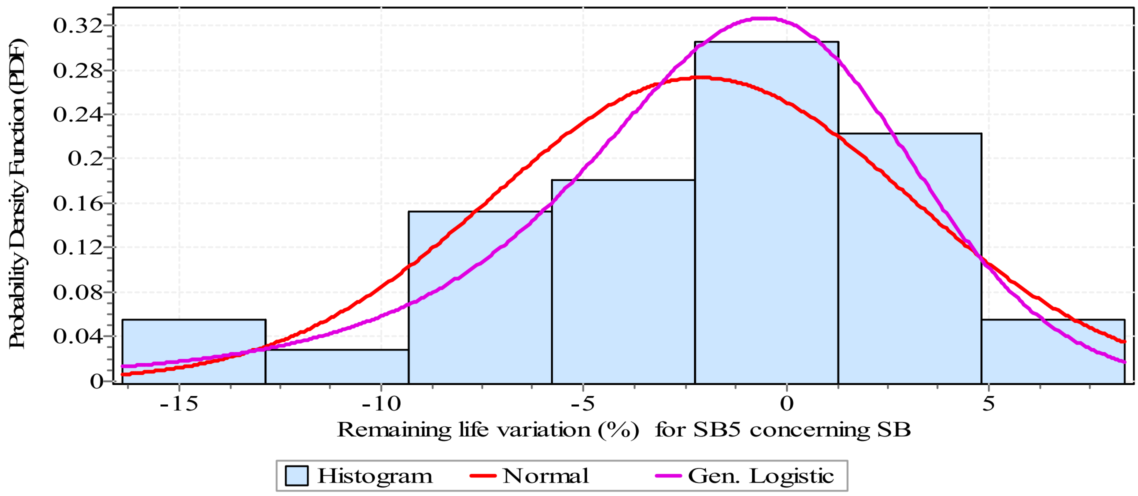

(b4) Variation in remaining life at 'SB5' concerning 'SB'

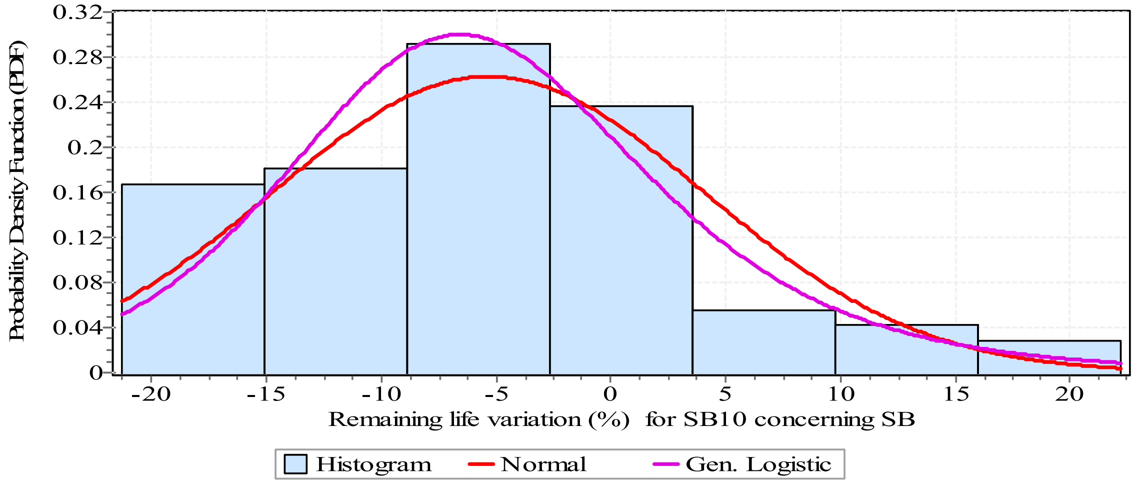

(b5) Variation in remaining life at 'SB10' concerning 'SB'

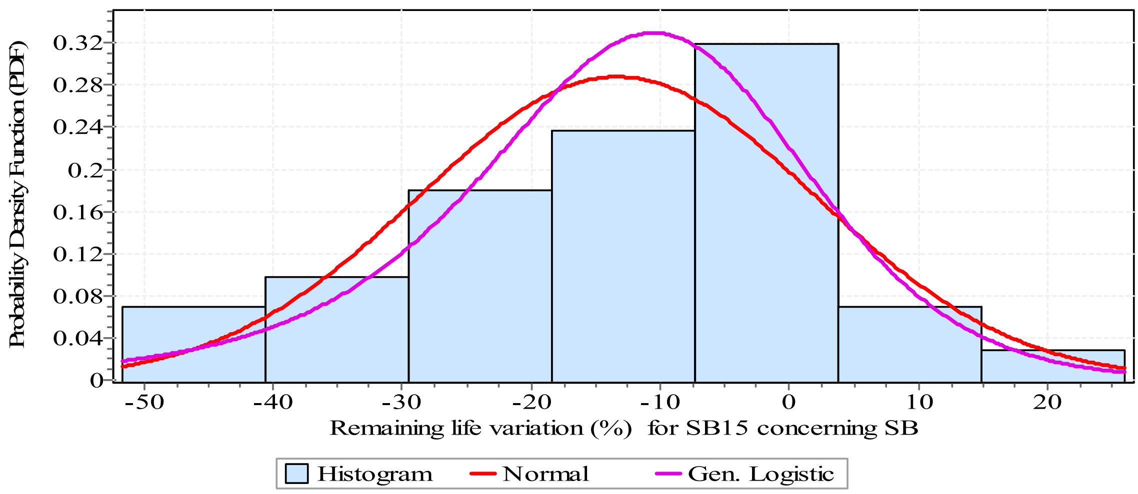

(b6) Variation in remaining life at 'SB15' concerning 'SB'

Figure 4.16(b): PVPD variation and remaining life variation histogram, best fit curve and normal distribution curve. [Major span]

Table 4.8 provides summary of variation due to different stress bands (SB5, SB10, and SB15) to stress band ('SB') for PVPD and remaining life. Eqn 4.3, 4.4, and 4.5 provide the equation for PDF for general, log-logistic, and generalized logistic distributions respectively. And Table 4.8 provides the parameters of these distributions. For PVPD, with reference to stress band 'SB', variation ranges from -18% to 40%, -40% to 68%, and -47% to 173% for SB5, SB10 and SB15 respectively. For remaining life, with reference to stress band 'SB', variation ranges from -16% to 8%, -21% to 22%, and -52% to 26% for SB5, SB10 and SB15 respectively.

Table 4.8: Statistical parameters of distributions for variation in PVPD and remaining life concerning stress band 'SB' [Major span]

Particular	Stress band	Lower limit (%)	Higher limit (%)	Parameters of best-fit distribution (log-logistic)			Parameters of normal distribution	
				(α)	(β)	(γ)	(σ)	(μ)
PVPD	SB5	-18.6	40.6	11.265	52.994	-51.15	8.713	2.4876
PVPD	SB10	-39.9	68.2	8.2872	77.808	-71.771	17.677	8.045
PVPD	SB15	-47.3	173.1	4.4876	90.854	-70.66	38.39	27.161
Particular	Stress band	Lower limit (%)	Higher limit (%)	Parameters of best-fit distribution (generalized-logistic)			Parameters of normal distribution	
				(k)	(σ_1)	(μ_1)	(σ)	(μ)
Remaining life	SB5	-16.4	8.3	-0.153	2.7641	-1.4001	5.1589	-2.1149
Remaining life	SB10	-21.3	22.2	0.065	5.1985	-5.8978	9.4311	-5.3392
Remaining life	SB15	-51.6	25.9	-0.0906	8.4652	-12.048	15.345	-13.321

The stringer (2508) is the most critical member of the major span, according to Table 4.7(b). If suggested future loading CC+8+2T run over the bridge at speed V1 with anticipated GMT and train combination each day Table 4.1(b), it might endure up to 65.6 years.

However, if a decision is made to run a future loading of 32.5T at speed V3, the same member may fail in 26.5 years.

It is important to mention here that remaining life obtained above is life of super structure and not the overall structure of the bridge. Since STAAD model of super structure is generated for remaining life assessment of the existing bridge.

4.9 Concluding remarks

4.9.1 Summary of minor span

1. The bridge's Minor span is examined using the stress-life approach while taking into account four various stress bands, three different speed conditions, and three futuristic loading scenarios.
2. The three most critical members of the minor span are the stringer (1504) at the end section, the X-beam (1618) at the midsection, and the diagonal L2U3 (1409) all based on the remaining life of the bridge members.
3. The remaining life of the stringer (1504) at the endsection, X-beam (1618) at the middle, and diagonal L2U3 (1409) varies from 18.4 to 60.5 years, 36.9 to 78.1 years, and 43.8 to 87.2 years, respectively, depending on the type of future loading adopted and the speed of trains run.
4. For a specific speed and stress band, the remaining life is lowest, between, and maximum for 32.5T loading, 25T loading, and CC+8+2T loading, respectively.
5. To provide an indication of the accuracy, the variation in remaining life and PVPD due to SB5, SB10, and SB15 with respect to SB are assessed. Since the stress band SB10 is frequently employed directly in practical situations.

6. It can be inferred from the normal distribution curve of the PVPD variation that the standard deviation of the variation with respect to 'SB' for SB5, SB10, and SB15 is 9.5%, 19.4%, and 30.4%, respectively, and the mean of variation with respect to 'SB' is 2.5%, 6.7%, and 13.8%, respectively.
7. It can be inferred from the normal distribution curve of the remaining life variation that the standard deviation of the variation with respect to 'SB' for SB5, SB10, and SB15 is 4.5%, 8.5%, and 18.9%, respectively, and the mean of variation with respect to 'SB' is -1.2%, -6.6%, and -5.5%, respectively.
8. The log-logistic and generalized-logistic distributions are the best-fit distributions for PVPD variation and remaining life variation for SB5, SB10, and SB15 concerning 'SB'.

4.9.2 Summary of major span

1. The stress-life approach is used to study the bridge's main span while taking into account four various stress bands, three different speed conditions, and three proposed or future loadings.
2. Based on the remaining life of the bridge members, the stringer (2508) at midsection, the diagonal L6M7 (2412), and the X-beam (2638) at midsection are, in that order, the three most important members of the major span.
3. The remaining life of the stringer (2508) at the midsection, the L6M7 (2412), and the X-beam (2638) at the midsection, respectively, varies from 26.5 to 65.6 years, 48.1 to 98.1 years, and 69.4 to 118.2 years, depending on the type of future loading adopted and the speed of trains run.
4. For a specific speed and stress band, the remaining life is lowest, between, and maximum for 32.5T loading, 25T loading, and CC+8+2T loading, respectively.

5. The variation in remaining life and PVPD owing to SB5, SB10, and SB15 in relation to SB is calculated to gain an indication of accuracy. Because, in most circumstances, stress band SB10 is used directly.
6. It can be inferred from the normal distribution curve of the PVPD variation that the standard deviation of the variation with respect to 'SB' for SB5, SB10, and SB15 is 8.7%, 17.7%, and 38.4%, respectively, and the mean of variation with respect to 'SB' is 2.5%, 8.0%, and 27.2%, respectively.
7. It can be inferred from the normal distribution curve of the remaining life variation that the standard deviation of the variation with respect to 'SB' for SB5, SB10, and SB15 is 5.2%, 9.4%, and 15.3%, respectively, and the mean of variation with respect to 'SB' is -2.1%, -5.3%, and -13.3%, respectively.
8. The log-logistic and generalized-logistic distributions are the best-fit distributions for PVPD variation and remaining life variation for SB5, SB10, and SB15 concerning 'SB'.

4.9.3 Conclusion

For particular speed and stress band, assessed remaining life is minimal, in between, and maximum for 32.5T loading, 25T loading, and CC+8+2T loading. The remaining life of the bridge varies from 18.4 to 60.5 years for the Minor span and from 26.5 to 65.6 years for the major span, depending on the type of future loading and its running speed over the concerned bridge. In case of per vehicle passage damage (PVPD) and remaining life, variation at wider stress band is more compare to narrower stress band concerning stress band ‘SB’. The best-fit distribution for PVPD variation for SB5, SB10, and SB15 is the log-logistic distribution. The generalized-logistic distribution is the best-fit distribution for variation in remaining life for SB5, SB10, and SB15. This study will be helpful in health assessment and timely maintenance of railway, highway, and rail-cum-roadway bridges.